Polarization of the Yeast Pheromone Receptor Requires Its Internalization but Not Actin-dependent Secretion

Dmitry V. Suchkov,[*][†] **Reagan DeFlorio,**[*][‡] **Edward Draper,**[‡][§] **Amber Ismael,**[*][‡] **Madhushalini Sukumar,**[*][‡] **Robert Arkowitz,**[‖] **and David E. Stone**[*]

[*]Laboratory for Molecular Biology, Department of Biological Sciences, University of Illinois at Chicago, Chicago, IL 60607; and [‖]Institute of Developmental Biology and Cancer Research, University of Nice, 06108 Nice Cedex 2, France

In the best understood models of eukaryotic directional sensing, chemotactic cells maintain a uniform distribution of surface receptors even when responding to chemical gradients. The yeast pheromone receptor is also uniformly distributed on the plasma membrane of vegetative cells, but pheromone induces its polarization into "crescents" that cap the future mating projection. Here, we find that in pheromone-treated cells, receptor crescents are visible before detectable polarization of actin cables and that the receptor can polarize in the absence of actin-dependent directed secretion. Receptor internalization, in contrast, seems to be essential for the generation of receptor polarity, and mutations that deregulate this process confer dramatic defects in directional sensing. We also show that pheromone induces the internalization and subsequent polarization of the mating-specific Gα and Gβ proteins and that the changes in G protein localization depend on receptor internalization and receptor–Gα coupling. Our data suggest that the polarization of the receptor and its G protein precedes actin polarization and is important for gradient sensing. We propose that the establishment of receptor/G protein polarity depends on a novel mechanism involving differential internalization and that this serves to amplify the shallow gradient of activated receptor across the cell.

INTRODUCTION

Chemotaxis, or directed cell movement in response to a gradient of chemoattractant or repellent, plays a vital role in development and immunity. For example, cell migration during embryogenesis is dependent on chemotaxis, as is wound healing, and the migration of leukocytes and macrophages to sites of tissue damage and infection (Iijima *et al.*, 2002). The related phenomenon of chemotropism—directed cell growth in response to a chemical gradient—is integral to axon guidance (Biber *et al.*, 2002; Rubel and Cramer, 2002), angiogenesis (Nern and Arkowitz, 1999; English *et al.*, 2001; Basile *et al.*, 2004), pollen tube guidance (Palanivelu and Preuss, 2000; Kim *et al.*, 2004), and fungal infection (Snetselaar *et al.*, 1996; Daniels *et al.*, 2006).

Interpreting and responding to a chemical gradient requires a set of attributes shared by all eukaryotic cells able to sense direction. Such cells display surface receptors that bind the chemoattractant. G protein-coupled receptors (GPCRs) are most commonly used for this purpose (Weiner, 2002). Because physiological gradients of chemoattractant are typically very shallow, 1–10% across the cell's length (Mato *et al.*, 1975; Tranquillo *et al.*, 1988; Segall, 1993),

the cell must be able to convert small differences in receptor occupancy into substantially steeper intracellular signaling gradients. These internally amplified molecular gradients ultimately determine the axis of polarity and define a polarity site or region at the cell cortex. Finally, the cell orients the actin and/or microtubule cytoskeletons toward the polarity site to promote movement or growth in that direction.

In the well studied chemotactic models such as *Dictyostelium* and mammalian neutrophils, the chemoattractant receptors are uniformly distributed on the cell surface and remain so even as cells respond to dynamic gradients (Xiao *et al.*, 1997; Servant *et al.*, 1999). The direction of movement is entirely determined by locally amplified intracellular signaling pathways that respond to the changing pattern of liganded receptor. It is easy to see the advantage of this design for migrating cells exposed to gradients that change on a second-to-minute time scale and which may frequently have to alter their heading.

By comparison, chemotropism is a very slow and committed response, in many cases lasting hours to days, so some mechanistic differences might be expected. Arguably the best characterized chemotropic response is the mating process of the budding yeast, *Saccharomyces cerevisiae*. In the haploid phase of its life cycle, budding yeast exist as two mating types, *MAT***a** and *MAT*α. Each mating type constitutively secretes a specific peptide mating pheromone that binds to GPCRs on cells of the opposite type. Activation of the associated heterotrimeric G protein triggers arrest in the G1 phase of the cell cycle, broad changes in gene expression, and morphogenesis. In mating mixtures, cells find and contact the closest potential mating partner by determining the direction of the most potent pheromone source and growing toward it (Jackson and Hartwell, 1990). This polarized

[‡] These authors contributed equally to this work.

Present addresses: [†] Cellecta Incorporated, Mountain View, CA 94043; [§] Center for Molecular Biology of Oral Diseases, University of Illinois at Chicago, Chicago, IL 60612.

Address correspondence to: David E. Stone (dstone@uic.edu).

growth is called a mating projection, and the pear-shaped cell, a "shmoo."

Polarized growth in *S. cerevisiae*, like that in higher eukaryotes, requires the marking of a growth site at the cell cortex and alignment of the actin cytoskeleton toward it. The actin cables serve as highways along which cargo bound for the polarized structures is transported by myosin motors (Pruyne and Bretscher, 2000a,b). Actin polarization depends on Cdc42, which is thought to activate a formin protein (Bni1) that nucleates and tethers actin cables to the polarization site (Evangelista *et al.*, 2002; Sagot *et al.*, 2002). Cdc42 is activated by the guanine nucleotide exchange factor, Cdc24, which itself undergoes localized activation by positional cues during both vegetative growth (budding) and mating. In vegetative cells, cortical tags promote localized activation of the Ras-related GTPase, Bud1/Rsr1 (hereafter Bud1), which binds directly to Cdc24. In mating cells, Gβγ interacts directly with Far1, which binds directly to Cdc24. Interaction of Gβγ with Far1 is thought to activate the bound Cdc24 (Wiget *et al.*, 2004), leading to localized guanosine triphosphate-loading of Cdc42, recruitment of Bni1, nucleation of actin cables, and polarized growth to form the mating projection. Under physiological conditions, the Gβγ–Far1 complex is presumed to assemble in the region of the cell surface that experiences the highest concentration of pheromone, and to mark this area for growth in preference to the predetermined bud site. Thus, the cell orients its growth toward the source of pheromone. In a pheromone gradient, formation of this Gβγ–Far1–Cdc24–Cdc42 chemotropic complex overrides formation of the Bud1–Cdc24–Cdc42 budding complex. When cells are unable to sense a gradient of pheromone, however, they form a mating projection at the site that would have been used for the next bud—the site marked by Bud1 (Dorer *et al.*, 1995; Nern and Arkowitz, 1999). This is called the default mating projection site, or default shmoo site.

Although many of the molecules and mechanisms that link external signals to the cytoskeleton and polarized secretion are similar in the yeast mating response and the chemotactic processes, one outstanding difference is the behavior of the receptors. Unlike the invariant distribution of chemotactic receptors, the pheromone receptors are dramatically redistributed upon stimulation. When vegetative cells expressing a green fluorescent protein (GFP)-tagged form of the α-factor receptor (Ste2-GFP) are treated with pheromone, the initially uniform fluorescent signal on the plasma membrane transiently disappears, then reappears as a polarized "cap" on the tip of the mating projection (Ayscough and Drubin, 1998; Moore *et al.*, 2008). This redistribution is thought to be driven by actin-dependent directed secretion and endocytosis but may also require actin-independent mechanisms such as receptor clustering. As an integral membrane protein, Ste2 is uniformly delivered to the plasma membrane in secretory vesicles during vegetative growth. In pheromone-treated cells, Ste2 is deposited at the shmoo site by vesicles moved along polarized actin cables by the myosin V motor protein Myo2. Ste2 is also subjected to actin-dependent endocytosis at both a basal mode and at a 5- to 10-fold faster ligand-induced rate (Jenness and Spatrick, 1986). The internalization of Ste2 is regulated by a pair of sister casein kinases, Yck1 and Yck2, which are required for phosphorylation of the receptor on its C-terminal cytoplasmic tail (Hicke *et al.*, 1998). Yck-dependent phosphorylation of the receptor triggers its ubiquitation and subsequent internalization (Hicke *et al.*, 1998).

Like chemotaxing cells, yeast exhibit a remarkable ability to interpret chemical gradients. It has been estimated that a 1% difference in receptor occupancy across the 4- to 5-μm length of a yeast cell in a pheromone gradient is sufficient to elicit robust orientation toward the pheromone source (Segall, 1993), and recent microfluidic studies suggest an even greater acuity (Moore *et al.*, 2008). How is this very slight gradient of activated receptor used to define the shmoo site? Does receptor polarization play an important role in establishing the axis of polarity? The polarized receptor crescent could represent the end point of a process that competes with Bud1 to establish the chemotropic shmoo site—in other words, the polarization of the pheromone receptor is a primary event in sensing the gradient and establishing the axis of polarity. Alternatively, the receptor crescent might simply be the result of directed secretion toward a growth site that was chosen before receptor polarization.

Here, we show that in cells subjected to isotropic pheromone treatment, receptor polarization does not depend on actin-dependent directed secretion and that receptor crescents are visible before detectable polarization of actin cables. Receptor internalization, in contrast, seems to be essential for the generation of receptor polarity, and mutations that deregulate this process confer dramatic defects in directional sensing. We also show that pheromone induces the internalization and polarization of the mating-specific Gα and Gβ proteins, and that the changes in G protein localization depend on receptor internalization and receptor–Gα coupling. Our data suggest a novel mechanism that contributes to growth site selection in pheromone gradients.

MATERIALS AND METHODS

Yeast Strains and Culture Conditions

The yeast strains used in this study are listed in Table 1. The GFP reporter strains were constructed by in situ tagging (Wach *et al.*, 1997) unless otherwise noted. *STE2* was tagged with GFP in situ in strains DSY257 (wild-type BF264-15D), BY4741, DLY6603 (*myo2-16*) and its isogenic control strain DLY6712 (MYO2), and LRB756 (*yck1Δ yck2-2*) by using HpaI-cut plasmid LHP1921 (see below) to create strains DMY169, DMY193, DMY226, DMY250, and DMY222, respectively. The *BUD1/RSR1* locus was deleted in strain DMY193 to create strain MSY163 using a *bud1Δ::URA3* cassette which was polymerase chain reaction (PCR) amplified from YCplac33 (Gietz and Sugino, 1988) by using the oligomers 5'-GCGCATTCATCCTCGACATTCTCAA-ACGCGAAATATCGTCGAACGTCTTCAAGAAATAGC-3' and 5'-GTTGT-GAAGTAGCGCTAATTCCTGTCCTGTTGCTAGAACCAGATTTCGCGATG-ATAAGCTGTCAAAC-3' as primers. *STE2* was GFP-tagged in situ in strain DLY5466 (*tpm1-2 tpm2Δ*) to create strain DMY232 using a PCR-based protocol: The kanamycin resistance gene was PCR amplified from pKT127-yEGFP-Kan (Sheff and Thorn, 2004) by using the oligomers 5'-GAAGCCAGAAAGT-TCTGGACTGAAGATAATAATAATTTAGGTGCTGGTTTAATTAAC-3' and 5'-CTTTGAAAAAGTAATTTCGTGACCTTCGGTATAAGGTTACATCG-ATGAATTCGAGCTCG-3' as primers, and the resulting PCR product was used to transform LRB756. Integrants were selected on YEPD plates supplemented with 200 mg/l G418 (Sigma-Aldrich, St. Louis, MO). *GPA1* was tagged with GFP in situ in strain DSY257 to create strain DMY235 using SphI-cut plasmid YIp128/Gpa1$^{Δ1-125}$-GFP (see below). The strains used to assess the effect of blocked receptor internalization on the localization of Gpa1 and Ste4 were created by transforming strain LHY848 (Ste2$^{K337R/340Stop}$) with YCplac22/GPA1-GFP (SLB156) and YCplac22/GFP-Ste4 (EDB121), respectively. The strain used to assess the localization Gpa1^{CTΔ5} was created by transforming strain MMY108 (Metodiev *et al.*, 2002) with the plasmid YCplac111/Gpa1^{CTΔ5}-GFP and plasmid Ycplac33/GPA1 was selected against in the presence of 5-fluoroorotic acid. The strain used to assess Ste4 localization in the absence of Gpa1 was created by the transforming *gpa1^{ts}* strain SZY136 (Zaichick *et al.*, 2009) with the plasmid pPR316-GFP-Ste4 (Kim *et al.*, 2009). Strain DMY171, used as a control in the partner discrimination assay, was created by transforming strain LHY10 (Shih *et al.*, 2000) with the StuI-cut plasmid pJR3 (Rohrer *et al.*, 1993). All yeast manipulations were performed as described previously (Sherman *et al.*, 1986).

Plasmid Construction

The plasmids used in this study are listed in Table 2. The key details of the newly constructed plasmids are described below. Recombinant DNA techniques were essentially as described previously (Ausubel *et al.*, 1994). Plasmid LHP1921 (from Linda Hicke, Department of Biochemistry, Molecular Biology

Table 1. Yeast strains used in this study

Strain	Background	Genotype	Source/reference
DSY257	BF264-15D	*MAT***a** *bar1Δ ade1 his2 leu2-3,112 trp1-1a ura3Δ*	Stone laboratory
DMY169	BF264-15D	*MAT***a** *bar1Δ ade1 his2 leu2-3 112 trp1 ura3 leu2:STE2-GFP::LEU2*	This study
BY4741		*MAT***a** GF(554) *his3D1 leu2D0 his3 met15D0 ura3D0*	Brachmann *et al.*, (1998)
DMY193	BY4741	*MAT***a** GF(554) *his3D1 leu2D0 his3 met15D0 ura3D0 leu2:STE2-GFP::LEU2*	Stone laboratory
MSY163	BY4741	*MAT***a** GF(554) *his3D1 leu2D0 his3 met15D0 ura3D0 leu2:STE2-GFP::LEU2 bud1Δ::URA3*	Stone laboratory
DMY167	LHY5112	*MAT***a** *ura3 leu2 his3 met15 leu2:STE2-GFP::LEU2*	Linda Hicke
DLY6603	ABY551	*MAT***a** *myo2-16::HIS3 bar1::URA his3D-200 leu2-2,112 lys2-801 trp1-1 ura3-52*	McNulty and Lew (2005)
DMY226	ABY551	*MAT***a** *myo2-16::HIS3 bar1::URA his3D-200 leu2-2,112 lys2-801 trp1-1 ura3-52 leu2:STE2-GFP::LEU2*	This study
DLY6712	ABY551	*MAT***a** *MYO2 bar1::URA his3D-200 leu2-2,112 lys2-801 trp1-1 ura3-52*	McNulty and Lew (2005)
DMY250	ABY551	*MAT***a** *MYO2 bar1::URA his3D-200 leu2-2,112 lys2-801 trp1-1 ura3-52 leu2:STE2-GFP::LEU2*	This study
LRB758		MATa *his3 leu2 ura3-52*	Panek *et al.*, (1997)
LRB758	DMY224	MATa *his3 leu2 ura3-52 leu2:STE2-GFP::LEU2*	
LRB756		MATa *his3 leu2 ura3-52 yck1-D1::ura3 yck2-2*[ts]	Panek *et al.*, (1997)
DMY222	LRB756	MATa *his3 leu2 ura3-52 yck1-D1::ura3 yck2-2*[ts] *leu2:STE2-GFP::LEU2*	This study
DLY5466	ABY971	*MAT***a** *tpm1-2::LEU2 tpm2D::HIS3 his3D-200 leu2-3 lys2-801 trp1-1 ura3-52*	Pruyne *et al.*, (1998)
DMY232	ABY971	*MAT***a** *tpm1-2::LEU2 tpm2D::HIS3 his3D-200 leu2-3 lys2-801 trp1-1 ura3-52 STE2-GFP::KanMX6*	This study
RDY126	BF264-15D	*MAT***a** *bar1Δ ade1 his2 leu2-3, 112 trp1 ura3 ste4::URA3 GFP-STE4::ura3*	This study
DMY235	BF264-15D	*MAT***a** *bar1Δ ade1 his2 leu2-3, 112 trp1 ura3 GPA1-GFP::LEU2*	This study
LHY848	LHY10	*MAT***a** *ste2::LEU2 ura3 leu2 his3 trp1 bar1-1 URA3::Ste2-337R-340Stop*	Shih *et al.*, (2000)
	LHY10	*MAT***a** *ste2::LEU2 ura3 leu2 his3 trp1 bar1-1 URA3::Ste2-337R-340Stop YCplac22/GPA1-GFP*	This study
	LHY10	*MAT***a** *ste2::LEU2 ura3 leu2 his3 trp1 bar1-1 URA3::Ste2-337R-340Stop YCplac22/GFP-Ste4*	This study
DMY238	BF264-15D	*MAT***a** *bar1Δ ade1 his2 leu2-3,112 trp1-1a ura3Δ gpa1::URA3*	This study
DMY239	BF264-15D	*MAT***a** *bar1Δ ade1 his2 leu2-3,112 trp1-1a ura3Δ gpa1*[ts] *pPR316-GFP-Ste4*	This study
DMY171	LHY10	*MAT***a** *ste2::LEU2 ura3 leu2 his3 trp1 bar1-1 URA3::STE2*	This study
YDB111		*MAT***a** *Sst2-GFP-KanMX6 Ste2*[7 × R]*-mCherry-caURA3Gpa1*[G302S]*-His3MX6*	Ballon *et al.*, (2006)
LHY844	LHY10	*MAT***a** *ste2::LEU2 ura3 leu2 his3 trp1 bar1-1 URA3::ste2-337R,340-UBIK48R*	Shih *et al.*, (2000)
8906-1-4b		*MAT*α *cry1 ade6 leu2 lys2 trp1 can1 ura3 SUP4*[a]	Schrick *et al.*, (1997)
8907-4-1b		*MAT*α *cry1 ade6 his4 leu2 tyr1 ura3 can1 cyh2 SUP4*[a] *mfb1::ura3*[FOA] *mfb2::LEU2*[a]	Schrick *et al.*, (1997)

and Cell Biology, Northwestern University) was constructed by fusing GFP in-frame to codon 419 of *STE2*. This eliminates the last 12 amino acids of Ste2 but leaves six of the seven C-terminal lysines. The unique HpaI site was removed from the GFP sequence by site-directed mutagenesis. YCplac22/GFP-Ste4 was constructed by subcloning the EcoRI-SmaI fragment containing the GFP-Ste4 fusion, which is under the control of the native *STE4* promoter, from plasmid pPR316-GFP-Ste4 (Kim *et al.*, 2000) into YCplac22 (Gietz and Sugino, 1988). YCplac22/Gpa1-GFP was constructed by subcloning the SalI-SacI fragment of pSLB126 (YCplac111/GPA1-GFP) containing the GPA1-GFP fusion, which is under the control of the native *GPA1* promoter, into YC-plac22. YIp128/Gpa1[Δ1-125]-GFP was created by subcloning the SalI-SacI fragment of pSLB126 (YCplac111/GPA1-GFP) into YIp128 (Gietz and Sugino, 1988) and then deleting the HindIII fragment containing the *GPA1* promoter and the first 374 nucleotides of the *GPA1* coding sequence. pRS316-CG/Gpa1[CTΔ5]-GFP

was created by amplifying the *GPA1* locus, including the promoter but lacking the last five codons, from a genomic template using the following primers: 5'-ACGCGTCGACAGGAAGCTGAAGTGCAAGGATTGA-3' and 5'-ATAA-GAATGCGGCCGCACTTTAAGGTTTTGCTGGATGATTAG-3'. SalI-NotI cut PCR product was then subcloned into pRS316-CG (Liu and Lindquist, 1999). YCplac111/Gpa1[CTΔ5]-GFP was constructed by subcloning the pRS316-CG/Gpa1[CTΔ5]-GFP SalI-SacI fragment containing the reporter fusion into YCplac111 (Gietz and Sugino, 1988). To construct plasmid GFP-Sec4 (from Nava Segev, Department of Biological Sciences, University of Illinois at Chicago), a XbaI-SacI genomic DNA fragment containing *SEC4* was PCR amplified and cloned into pRS315 (Sikorski and Hieter, 1989). yEGFP PCR-amplified from pKT127-yEGFP-Kan (Sheff and Thorn, 2004) was then inserted at the unique PciI site immediately upstream of the *SEC4* coding sequence, creating an in-frame GFP-Sec4 translational fusion.

Table 2. Plasmids used in this study

Plasmid no.	Plasmid name	Marker/plasmid type	Source
LHP1921	Ste2[1-419]-GFP	LEU2/INT	Dunn *et al.*, (2004)
PNS1227	pRS315/GFP-Sec4	LEU2/CEN	Nava Segev
SLB285	YIp128/Gpa1[Δ1-125]-GFP	LEU2/INT	This study
SLB156	YCplac22/GPA1-GFP	TRP1/CEN	This study
EDB121	YCplac22/GFP-Ste4	TRP1/CEN	This study
DMB153	YCplac111/Gpa1[CTΔ5]-GFP	LEU2/CEN	This study
pJR3	YIplac211/Ste2	URA3/INT	Rohrer *et al.*, (1993)

Cell Cycle Synchronization

Yeast cultures to be synchronized by centrifugal elutriation were grown in 1 l of synthetic medium containing 2% sucrose and 0.1% dextrose at 30 or 23°C for temperature-sensitive mutants to a density of 1×10^7 cells/ml. The cultures were then sonicated for 1 min at 50% power using a Braun Sonic U equipped with a microprobe, and loaded into the elutriation chamber of a JE-5.0 elutriation rotor in a Beckman J-6 M/E centrifuge (Beckman Coulter, Fullerton, CA). Elutriations were performed at 20°C using growth medium. Small cells without buds (newly abscised daughters) were collected at a rotor speed of 2700 rpm and a flow rate of 30 ml/min in a volume of 50–100 ml; they were kept on ice for no more than 1 h before being resuspended in fresh medium. The eluted samples invariably contained ≥95% G1 (undbudded) cells as judged by phase-contrast microscopy at 400× magnification. Because the GFP-Ste4 signal is significantly stronger in cells grown on solid rather than liquid media, G1-synchronized RDY126 cells were collected as described previously (Zhang *et al.*, 2001). In brief, 0.2 ml of overnight liquid culture was spread onto rich medium plates and incubated for 2 d at 30°C. Approximately 50 µl of cells was then transferred from the plates into 1 ml of 1 M sorbitol/0.5× YEPD, and spun for 1 min at 1000 × *g* to pellet the budded cells. The supernatant, enriched in unbudded cells, was collected and the process repeated until a sample containing ≥95% unbudded cells was obtained.

Fluorescent Microscopy

Fluorescent images for experiments carried out in liquid cultures were acquired using an Axioskop 2 microscope (Carl Zeis,, Jena, Germany) fitted with a 63× oil immersion objective (total magnification, 630×) and an Axio-Cam digital camera (Carl Zeiss), and processed with AxioVision software (Carl Zeiss). Images were analyzed and further processed using Photoshop 5.5 (Adobe Systems, San Jose, CA) and/or ImageJ (National Institutes of Health, Bethesda, MD).

Time-Lapse Fluorescent Microscopy in Mating Mixtures

Wild-type BF264-15D *MATα* cells were stained with 10 µg/ml ConA-Alexa Fluor 594 (Invitrogen, Carlsbad, CA) for 1 h and then washed three times with water before mixing with strain DMY167 (*MAT***a** cells that express STE2-GFP). Mating mixtures were incubated at 30°C on agar pads and images were acquired 30 min after mixing and at 20-min intervals thereafter. Six fields were imaged at each time point with six differential interference contrast (DIC) and six GFP Z-stacks collected in 0.4-µm slices using a DeltaVision deconvolution microscopy system (Applied Precision, Issaquah, WA) on an Olympus IX-70 microscope with a numerical aperture 1.4, 60× objective. The images were then deconvolved, sum projected (GFP) or average projected (DIC), and then converted into 8-bit TIF files images using Huygens Deconvolution Software (Scientific Volume Imaging, Hilversum, The Netherlands).

GFP Reporter Localization Studies in Liquid Cultures

Cells expressing GFP-tagged genes were grown to mid-log phase in rich medium (integrated reporters) or selective medium (cen-vector borne reporters) and treated with mating pheromone (α-factor). Pheromone doses, the addition or omission of latrunculin A (LatA), growth temperatures, and time points are indicated in the figure legends. Cells were collected by centrifuging 50- to 200-µl aliquots of culture and resuspending in 10–50 µl of phosphate-buffered saline (PBS). Fluorescent images were acquired as described above. For each experiment, localization of the GFP reporter was assessed in at least two transformants. ImageJ (Rasband, 1997–2009) was used to analyze the data. The outline of each cell was traced using the "segmented line" feature and the intensity of the fluorescent signal around the cell periphery was quantified using the "plot profile" function. Internal fluorescence intensity was obtained by selecting the interior of the cell, including all organelles, with the "brush" selection tool. The mean fluorescence intensity in the selected area was quantified using the "measure" function. The data for each cell was pasted into Excel files (Microsoft, Redmond, WA) programmed to calculate the degree of GFP-reporter polarization (the polarity index) and the ratio of plasma membrane to intracellular GFP-reporter signal (plasma membrane/cytoplasm). The polarity index was obtained by dividing the mean signal intensity in the brightest quarter of the plasma membrane by the mean signal intensity in the rest of the plasma membrane. The ratio of cytoplasmic to intracellular fluorescence was obtained by dividing the mean fluorescence intensity at the plasma membrane by the mean fluorescence intensity inside the cell. Only randomly selected unbudded cells were scored.

Actin Staining

F-actin was stained essentially as described previously (Pringle *et al.*, 1989).

Partner Discrimination Assay

Mating partner discrimination assays were performed essentially as described previously (Schrick *et al.*, 1997) using the tester strains described therein. Each mating mixture contained ~2×10^5 *MAT***a** cells, 2×10^5 *MATα* pheromone secretors, and 4×10^6 *MATα* nonsecretors. Thus, the ratio of pheromone secretors to nonsecretors was 1:20.

RESULTS

In Mating Mixtures, the Receptor Polarizes before Morphogenesis and Orients toward the Closest Mating Partner

In previous studies of receptor localization, pheromone-induced polarization was seen at the shmoo tip but was not noted before mating projection emergence (Jackson *et al.*, 1991; Ayscough and Drubin, 1998). If receptor polarization plays an important role in establishing the axis of polarity, it must occur before morphogenesis and must coincide with the future chemotropic shmoo site. To examine these possibilities, we took time-lapse DIC and fluorescent images of mating cultures in which wild-type *MAT***a** cells expressing Ste2-GFP were mixed with *MATα* cells labeled with concanavalin A (ConA) Alexa Fluor 594. As reported previously (Jackson *et al.*, 1991; Ayscough and Drubin, 1998), the Ste2-GFP reporter was uniformly distributed on the plasma membrane of vegetative cells and seemed to be internalized upon exposure to pheromone (data not shown). However, time-lapse images revealed the development of receptor polarity well before mating projection formation (Figure 1A). In fact, polarized receptor "crescents" appeared on the membranes of unbudded cells before they exhibited any obvious change in shape (Figure 1B). Moreover, the formation of polarized receptor crescents was clearly a chemotropic response: Of the *MAT***a** cells that were positioned less than two cell lengths from *MATα* partners, 82% (36/44) formed detectable receptor crescents and 100% of these crescents were oriented toward the closest mating partner. If receptor polarization occurs after selection of the shmoo site, the receptor crescent might orient away from the mating partner at first and then reorient toward it. On the contrary,
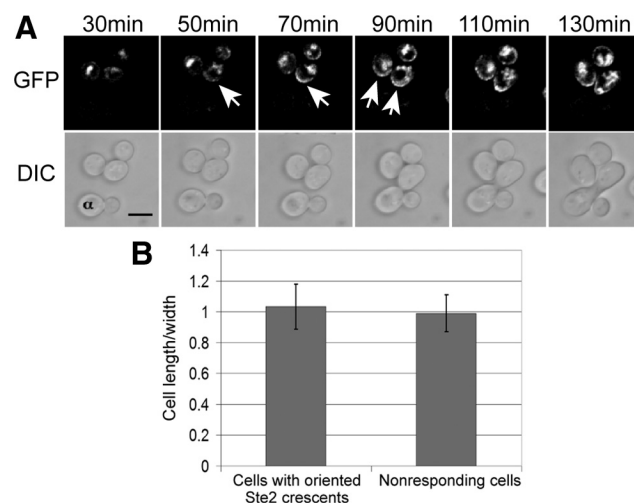

Figure 1. Receptor crescents form on the up-gradient side of the plasma membrane. (A) Wild-type *MAT***a** cells expressing Ste2-GFP (strain DMY169) were mixed with congenic *MATα* cells prestained with ConA-Alexa Fluor 594 (labeled α) and incubated on agar pads at 30°C for 30 min. Fluorescent (top) and DIC (bottom) images were then acquired every 20 min. Arrows indicate Ste2-GFP crescents. Bar, 5 µm. (B) Pheromone-induced morphogenesis. The bar graphs represent the mean ratio ± SD of cell length to maximal width. Two populations of cells were measured. For cells responding to a proximal mating partner, cell length was measured along the axis of polarity at the time point that the Ste2-GFP crescent was first visible (n = 36). As a control, randomly chosen nonresponding cells were measured along their vertical and horizontal axes (n = 36). There was no significant difference in the shape of the responding and nonresponding cells (p = 0.31).

we found that receptor crescents were always oriented toward the nearest partner upon emergence. Either reorientation occurs before the crescent can be detected, or polarized receptor distribution is established early and in response to the pheromone gradient, consistent with a role for receptor polarity in establishing the shmoo site.

Receptor Polarization Induced by Isotropic Pheromone Treatment Is Similar to That Seen in Mating Mixtures and Does Not Depend on Bud1

Because quantifying the early polarization of Ste2-GFP in multiple mating pairs was not possible due to technical obstacles, we investigated the mechanisms underlying receptor polarization in cells subjected to isotropic pheromone treatment. Wild-type strain DMY169 was grown to mid-log phase and small G1 cells (newly abscised daughters) were collected by centrifugal elutriation, then treated with pheromone or allowed to proliferate in liquid culture. Aliquots

were taken at intervals to acquire fluorescent images of live cells and to fix cells for actin staining. The GFP signal around the perimeter and in the cytoplasm of randomly chosen cells was quantified and Ste2-GFP polarization was assessed by determining the ratio of the mean fluorescence in the brightest one quarter of the membrane to mean fluorescence around the rest of the perimeter, which reflects the distribution of the reporter around the plasma membrane. We also determined the ratio of the mean plasma membrane to mean cytoplasmic signals. Because nascent GFP molecules are not competent to fluoresce for at least 15 min (Gordon *et al.*, 2007), this measure largely reflects the removal of Ste2-GFP from membrane and its accumulation in the vacuole during the first 15 min after pheromone treatment. Actin was visualized in the fixed cells by Alexa Fluor 594 phalloidin (Invitrogen) staining.

Isotropic pheromone treatment of DMY169 cells growing in liquid medium induced similar changes in Ste2-GFP lo-

Figure 2. Receptor localization in synchronized cells. (A) Representative fluorescent images of Ste2-GFP localization and F-actin in wild-type strain DMY169. G1-synchronized cells were treated with 30 nM α-Factor (αF) pheromone (0 time) or cultured without pheromone as indicated, and images were acquired every 15 min. Arrows indicate Ste2-GFP crescents. (B) Quantification of Ste2-GFP polarization. The degree of Ste2-GFP polarization in a given cell (the polarity index) was obtained by dividing the mean signal intensity in the brightest quarter of the plasma membrane by the mean signal intensity in the rest of the plasma membrane. The bar graphs represent the mean polarity index $\pm$ SD at each time point (n = 15). *$p < 0.0001$ for the comparisons of treated to untreated cells at each time point. (C) Ratio of plasma membrane to intracellular Ste2-GFP signal. The relative degree of Ste2-GFP membrane localization was obtained by dividing the mean fluorescence intensity at the plasma membrane by the mean fluorescence intensity inside the cell. The bar graphs represent the mean ratio $\pm$ SD of the plasma membrane to cytoplasmic signals at each time point (n = 15). *$p < 0.0001$ for the comparison treated to untreated cells. (D) Quantification of polarized actin cables. Cells stained with Alexa Fluor 594 Phalloidin (A, bottom line) were scored as having disorganized or polarized actin cables. The bar graphs represent the percentage of cells in each category at each time point (n $\geq$ 23); Cells in which actin cables were not detectable make up the remaining fraction of the population, and are not shown. The percentages of cells with clearly visible receptor crescents (polarity index $\geq$1.7) at each time point are also indicated on the graph (n $\geq$ 18). (E) Pheromone-induced morphogenesis. The bar graphs represent the mean ratio $\pm$ SD of cell length to maximal width (n = 20 for each time point). These cells did not significantly elongate until between 45 and 60 min after pheromone treatment (For the comparison treated to untreated cells, p = 0.142 at 45 min and *$p < 0.0002$ at 60 and 90 min.).
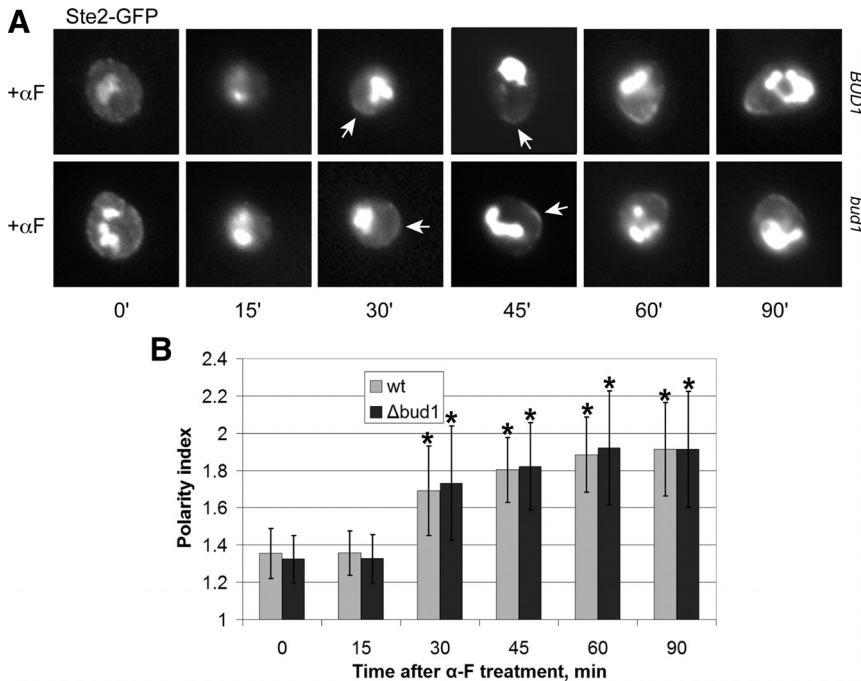
A Ste2-GFP

B
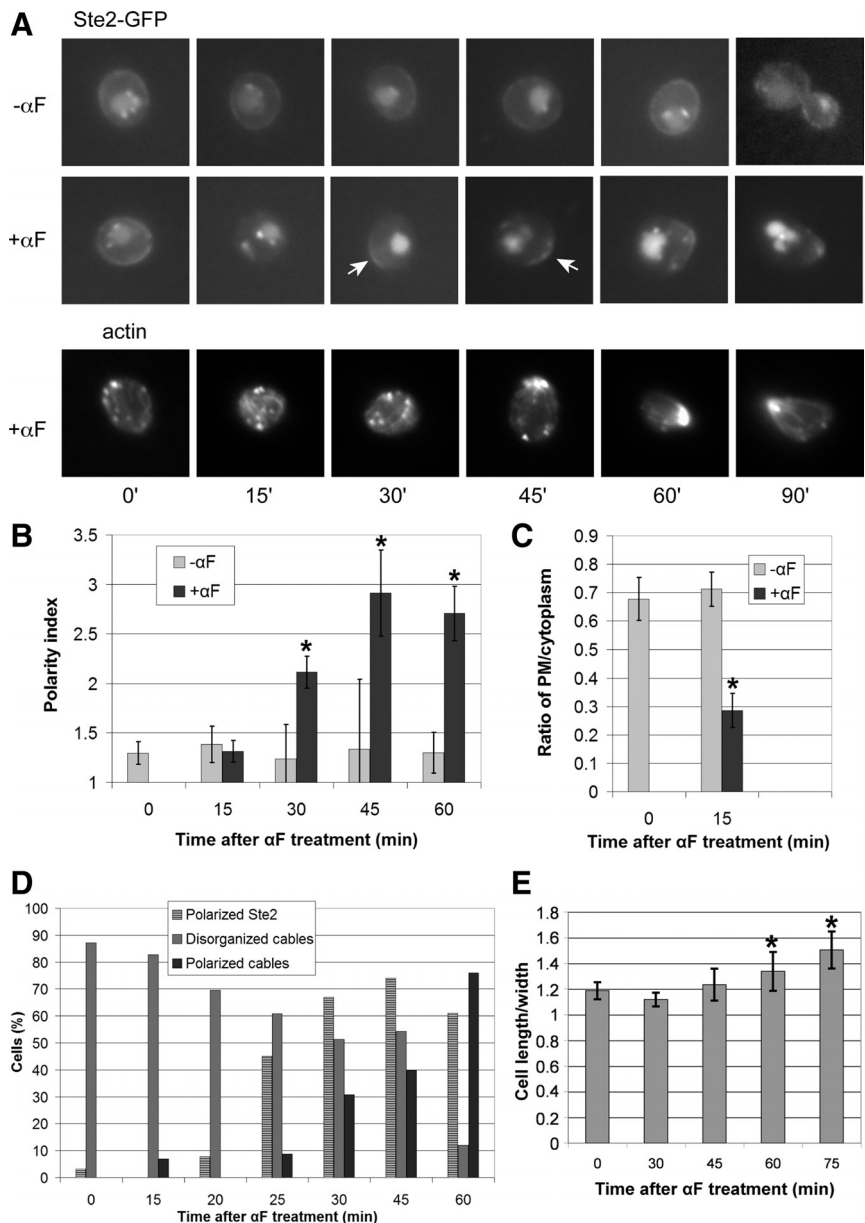
Figure 3. Receptor localization in synchronized *bud1*Δ cells. (A) Representative fluorescent images of Ste2-GFP localization *bud1*Δ strain MSY163. G1-synchronized cells were treated with 30 nM α-Factor (αF) pheromone (0 time), and images were acquired every 15 min. Arrows indicate Ste2-GFP crescents. (B) Quantification of Ste2-GFP polarization. The degree of Ste2-GFP polarization in a given cell (the polarity index) was obtained as described in Figure 2. The bar graphs represent the mean polarity index ± SD at each time point (n = 15). *$p < 0.0001$ for the comparisons of treated to untreated cells at each time point.

calization to those observed in mating cells (Figure 2A). Quantification of the Ste2-GFP signal in G1-synchronized cells yielded conclusions consistent with the established picture of receptor localization (Figure 2, B and C): 1) The pheromone receptor was almost uniformly distributed on the plasma membrane in vegetative cells and its localization was not cell cycle dependent. 2) Pheromone induced a dramatic drop in the membrane signal and a corresponding increase in the vacuolar signal in the first 15 min after treatment. 3) The receptor became significantly polarized within 30 min after treatment. Notably, polarized receptor crescents were visible well before detectable polarization of actin cables and polarized growth (Figure 2, A, D, and E).

Because cells exposed to a saturating or uniform concentration of pheromone shmoo by the default pathway, i.e., the mating projection is formed where the cell was going to bud (Dorer *et al.*, 1995), we wondered whether cells unable to mark the bud site could form receptor crescents in response to isotropic pheromone treatment. As shown in Figure 3, *bud1*Δ cells exhibited no measurable defect in receptor polarization. This demonstrates that cells can polarize the pheromone receptor in the absence both of a directional signal and the default polarization pathway.

Actin-dependent Directed Secretion Is Not Essential for the Formation of Receptor Crescents

The growth of the mating projection is due to the polarized delivery and fusion of vesicles containing plasma membrane and cell wall constituents. These vesicles are transported along actin cables oriented toward the shmoo site by Myo2. Ste2 and other signaling molecules are thought to be carried to the shmoo tip in the same way, and this mechanism is expected to contribute to the polarized distribution of the receptor as the cell elongates. However, it is not clear whether directed secretion is required to establish receptor polarity or merely to amplify it. This distinction cannot be definitively made by simple imaging experiments such as that shown in Figure 2 because the temporal relationship between the appearance of receptor crescents and polarized

actin unavoidably depends on the relative sensitivity of the methods for detecting the receptor and F-actin. Therefore, to determine whether formation of the receptor crescent depends on actin-dependent directed secretion, we imaged and quantified Ste2-GFP in mutant cells unable to transport vesicles to the cell surface via actin cables.

The Myo2-16 mutant protein is conditionally defective in transporting secretory vesicles (Schott *et al.*, 1999). When shifted to restrictive temperature (33°C), *myo2-16* cells rapidly lose the ability to target these vesicles to growth sites, and are therefore unable to polarize their growth (Schott *et al.*, 1999; Figure 4A). Nevertheless, the initial polarization of Ste2-GFP was detectable under these conditions: The *myo2-16* cells were able to form receptor crescents at 37°C, although these were less pronounced and less stable than the crescents produced by the mutant cells cultured at permissive temperature and by the isogenic *MYO2* control cells cultured at restrictive temperature (Figure 4, A and B). The induction of receptor polarity observed in the *myo2-16* strain is not likely due to residual Myo2 function, as GFP-Sec4, a sensitive reporter of directed secretion, showed no evidence of polarization under identical conditions (Figure 4, A and B) and in similar experiments (Sheltzer and Rose, 2009), nor was there any evidence of actin polarity (Figure 4, A and B). Similarly, the loss of tropomyosin function, which leads to the rapid disappearance of actin cables and an inability to either bud or shmoo (Pruyne *et al.*, 1998), did not prevent the formation of Ste2-GFP crescents (Figure 5). These data suggest that although actin-dependent directed secretion is necessary for the maintenance of receptor polarity, it is dispensable for its establishment.

Receptor Internalization and Casein Kinase Activity Are Essential for the Formation of Receptor Crescents and Directional Sensing

As discussed above, the pheromone receptor is phosphorylated, ubiquitinated, and internalized at a low constitutive level that is up-regulated 5- to 10-fold in response to pheromone stimulation (Jenness and Spatrick, 1986). Mutations
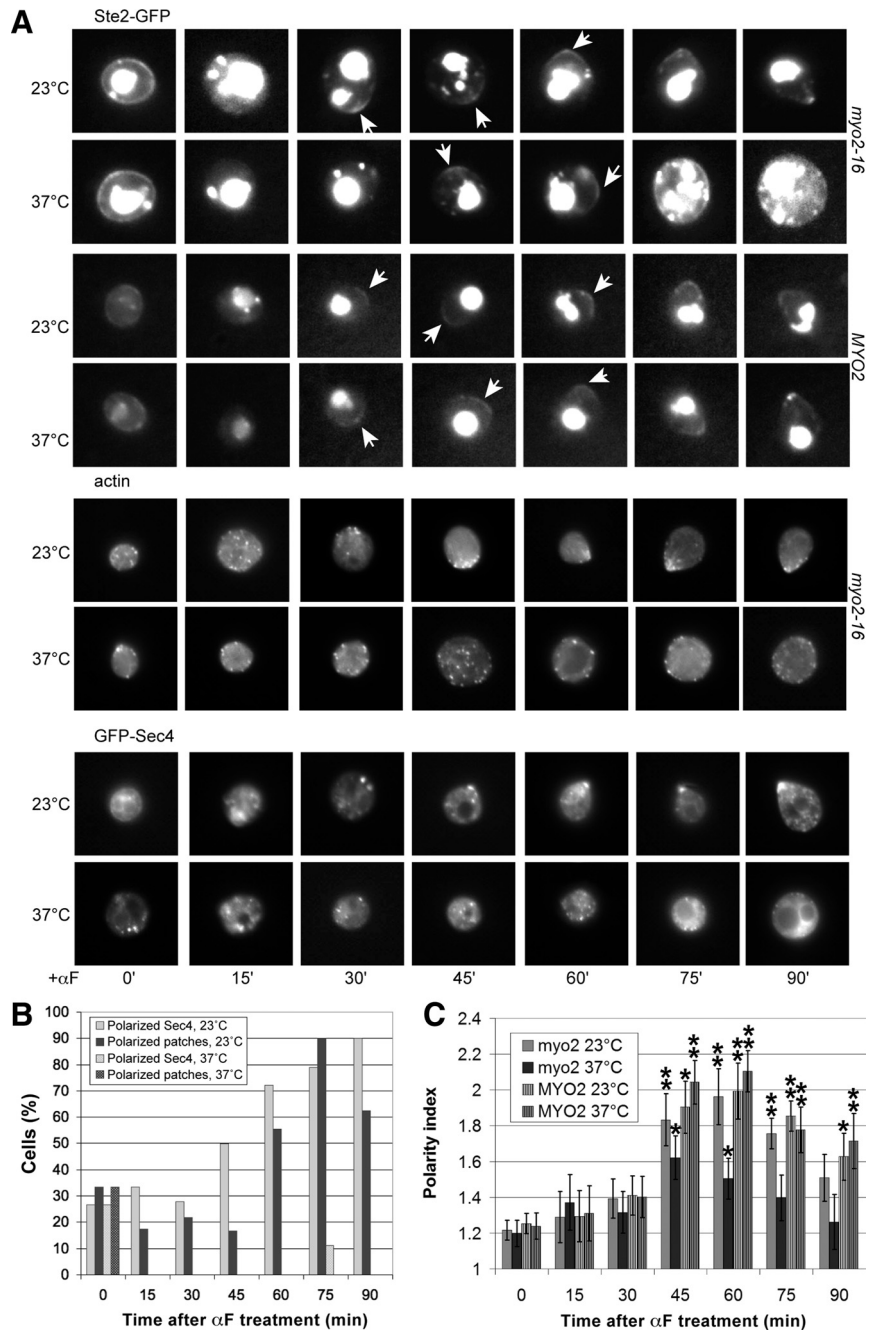
Figure 4. The receptor can polarize in the absence of Myo2 function. (A) Representative fluorescent images of Ste2-GFP localization, F-actin polarity, and GFP-Sec4 polarization in *myo2* temperature-sensitive and *MYO2* isogenic control strains. G1-synchronized cells were treated with 30 nM pheromone at the permissive temperature (0 time for the 23°C cultures) or 5 min after the shift to restrictive temperature (0 time for the 37°C cultures). Images were acquired every 15 min. Arrows indicate Ste2-GFP crescents. (B) Quantification of Sec4-GFP and actin patch polarity in *myo2-16* and *MYO2* cells at the permissive and restrictive temperatures. The bar graphs represent the percentages of cells exhibiting clear Sec4-GFP (light gray) and actin patch (dark gray) polarity at each time point ($32 \geq n \geq 8$). At 37°C, none of the cells showed actin patch polarity and only one cell showed Sec4-GFP polarity. (C) Quantification of Ste2-GFP polarization in *myo2-16* and *MYO2* cells at the permissive and restrictive temperatures. The bar graphs represent the mean polarity index ± SD at each time point (n = 15). *p < 0.001 and **p < 0.0001 for the comparisons of treated cells to 0 min.

that prevent the phosphorylation and/or ubiquitination of the receptor block its internalization (Reneke *et al.*, 1988) and confer a defect in adaptation to pheromone (Konopka *et al.*, 1988; Reneke *et al.*, 1988), but they do not disrupt its signaling functions (Konopka *et al.*, 1988). For example, the Ste2[K337R/340Stop] mutant form of the receptor, in which arginine has been substituted for lysine 337 and position 340 has been changed to a Stop codon, cannot be internalized but is still able to bind pheromone and induce cell cycle arrest and shmooing (Terrell *et al.*, 1998; Shih *et al.*, 2000). Inactivation of the casein kinase pair Yck1 and Yck2, which prevents phosphorylation of Ste2 and consequently its ubiquitination and internalization, phenocopies the effects of Ste2[K337R/340Stop] in pheromone-treated cells (Hicke *et al.*, 1998).

To determine whether formation of the receptor crescent depends on receptor internalization, we tagged Ste2[K337R/340Stop] with GFP in situ and quantified its localization in the same way we analyzed the wild-type receptor. As expected, pheromone did not induce internalization of Ste2[K337R/340Stop]-GFP, but notably, the distribution of Ste2[K337R/340Stop]-GFP on the plasma membrane also remained unchanged. The cells showed no evidence of receptor polarization even when they began to shmoo (Figure 6, A and B). Consistent with the behavior of Ste2[K337R/340Stop]-GFP, the wild-type Ste2-GFP reporter failed both to internalize and to polarize in *yck1Δ yck2[ts]* cells treated with pheromone at restrictive temperature and therefore lacking all Yck1/Yck2 activity (data not shown). When pheromone-treated *yck1Δ yck2[ts]* cells were allowed to endocytose the receptor until no de-
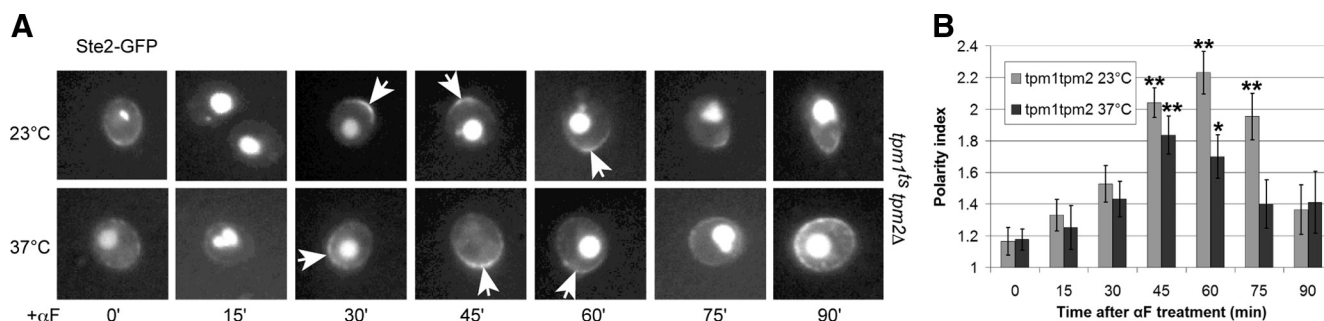
A

Ste2-GFP

B

Figure 5. The receptor can polarize in the absence of tropomyosin function. (A) Representative fluorescent images of Ste2-GFP localization in *tpm1-2 tpm2* temperature-sensitive cells. G1-synchronized cells were treated with 30 nM pheromone at the permissive temperature (0 time for the 23°C cultures) or 5 min after the shift to restrictive temperature (0 time for the 37° cultures). Images were acquired every 15 min. Arrows indicate Ste2-GFP crescents. (B) Quantification of Ste2-GFP polarization in *tpm1-2 tpm2-2* cells at the permissive and restrictive temperatures. The bar graphs represent the mean polarity index $\pm$ SD at each time point (n = 15). *$p < 0.01$ and **$p < 0.001$ for the comparisons of treated cells to 0 min.

tectable Ste2-GFP signal remained on the plasma membrane before being shifted to restrictive temperature, they were still unable to form Ste2-GFP crescents, whereas the isogenic *YCK1 YCK2* control cells formed robust crescents under these conditions, indicating that the generation of detectable receptor polarity requires ongoing Yck1/2 function (Figure 6C). These data suggest that in contrast to directed secretion of the receptor, its phosphorylation and internalization are essential for its pheromone-induced polarization.

Not surprisingly, cells that could not internalize and polarize their receptors—either due to mutation of the receptor (Ste2$^{K337R/340Stop}$) or the casein kinases (*yck1Δ yck2^{ts}*)—exhibited significant defects in directional sensing, as measured by the partner discrimination assay (Table 3). This correlation is consistent with the idea that receptor polarization plays a primary role in chemotropic growth site selection.

Actin-independent Mechanisms Contribute to Receptor Polarization

Our observation that receptor crescents form in the absence of actin-dependent directed secretion can be explained in several ways. If pheromone-induced endocytosis is not uniform, for example, we would expect the receptor and/or other polarity markers to become asymmetrically distributed as they are internalized. Alternatively, nascent receptors might be concentrated in a discrete area of the plasma membrane by actin-independent mechanisms. It has recently been reported that refed quiescent cells lacking functional actin cables and patches, due to LatA treatment or mutation, are nevertheless able to form terminal buds at premarked cortical sites (Sahin *et al.*, 2008). Although these buds are fragile and have wide necks, their existence demonstrates that polarized growth can occur by actin-independent mechanisms. Mutant cells unable to form actin cables can also form small buds when released from pheromone arrest (Bettinger *et al.*, 2007). A proposed explanation for these observations is that in cells lacking actin cables and patches, secretory vesicles move uniformly toward the plasma membrane but preferentially dock and fuse at sites where polarity cues are localized (Sahin *et al.*, 2008). In contrast, a mutational study has shown that vegetative cells require actin-dependent endocytic recycling functions to bud in the absence of actin cables (Yamamoto *et al.*, 2010).

To determine whether cells can form polarized receptor crescents in the complete absence of F-actin, we subjected wild-type cells expressing Ste2-GFP to concomitant LatA

and pheromone treatment. As shown in Figure 7, cells treated with LatA at zero time showed no sign of internalizing or polarizing the receptor. This is not surprising given that LatA blocks endocytosis and given our finding that cells unable to internalize the receptor seem unable to polarize it. Interestingly, however, wild-type cells treated with LatA 15 min after pheromone treatment—i.e., cells allowed to respond to pheromone with actin-dependent functions intact until almost no Ste2-GFP was detectable on their plasma membranes—formed robust receptor crescents over the next 30 min of pheromone stimulation, even though the delayed LatA treatment completely blocked their ability to polarize their growth (Figure 7, A and B) and to polymerize actin (data not shown). Delivery of the receptor to the membrane did apparently continue under these conditions, as the ratio of the plasma membrane to cytoplasmic Ste2-GFP signal increased in both cultures over time (Figure 7C). These data indicate that the generation of receptor polarity occurs in two empirically separable phases: an actin-dependent phase during which time the receptor is internalized, and an actin-independent phase during which time polarized receptor crescents manifest.

Pheromone Induces Asymmetric Receptor Phosphorylation in Cells That Cannot Polarize Receptor Localization

What happens during the initial, actin-dependent phase of the pheromone response that is obligatory to the appearance of actin-independent receptor crescents? A best guess generic answer is that a particular protein or set of proteins localizes to a patch of membrane where it serves as the polarity cue that biases vesicle fusion as postulated by Sahin *et al.* (2008). Cdc42 is a good candidate to play this role as it has been implicated in symmetry breaking (Kozubowski *et al.*, 2008) and its polarity is compromised in cells treated with both pheromone and LatA (Ayscough and Drubin, 1998). A second, but not mutually exclusive, possibility is that the receptor acts as a polarity cue, perhaps contributing to the polarization of Cdc42 via its interactions with G$\beta\gamma$, Far1, and Cdc24.

How might the receptor polarize during its actin-dependent global internalization phase, before actin cable-dependent directed secretion? In principle, receptor internalization could play a role in this process. It has been shown that pheromone binding triggers receptor phosphorylation and internalization in a G protein-independent manner (Zanolari *et al.*, 1992). If, however, an ele-
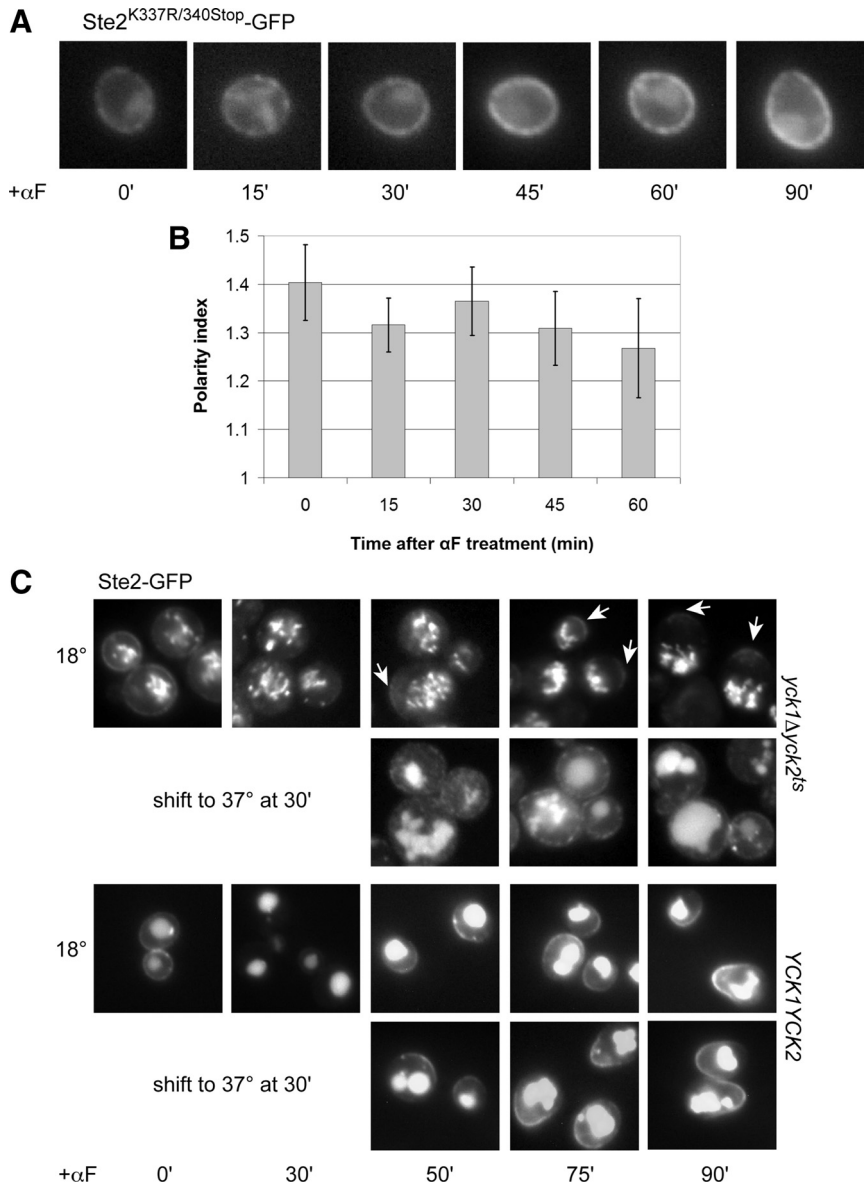
A   Ste2^{K337R/340Stop}-GFP

+αF   0'   15'   30'   45'   60'   90'

B

C   Ste2-GFP

+αF   0'   30'   50'   75'   90'

Figure 6. Pheromone-induced polarization of the receptor requires its internalization. (A) Representative fluorescent images of Ste2^{K337R/340Stop}-GFP localization. G1-synchronized cells were treated with 30 nM pheromone (0 time), and images were acquired every 15 min. (B) Quantification of Ste2^{K337R/340Stop}-GFP polarization. The bar graphs represent the mean polarity index ± SD at each time point (n = 15). (C) Representative fluorescent images of Ste2-GFP localization in yck1Δ yck2^{ts} mutant and YCK1 YCK2 isogenic control strains. Cells were grown to mid-log phase at 18°C and treated with 600 nM pheromone (0 time) for 30 min to allow for the initial internalization of the receptor. Half the culture was then shifted to the restrictive temperature (37°C), and images were acquired at the indicated time points. Arrows mark the Ste2-GFP crescents. None of the mutant cells cultured at restrictive temperature displayed detectable crescents (n = 66 at 75 min; n = 84 at 90 min), whereas polarized localization of Ste2-GFP was clearly visible in about a third of the yck1Δ yck2^{ts} cells cultured at the permissive temperature (33%, n = 106 at 75 min; 31%, n = 101 at 90 min).

ment activated or recruited by the liganded receptor could inhibit receptor phosphorylation and internalization, then receptors in the membrane region of highest signaling activity would be the least likely to be removed from the membrane, thereby creating a positive feedback loop. By inhibiting its own internalization, the activated receptor would begin to accumulate in the most active signaling area, leading to even greater protection and buildup of the receptor at what will become the shmoo site. As a first test of this hypothesis, we asked whether pheromone-induced phosphorylation of the receptor—the first step in the internalization pathway—is asymmetric.

To assay receptor phosphorylation in situ, we used strain YDB111, which expresses another mutant form of the receptor that cannot be internalized (Ste2^{7XR}-mCherry) instead of Ste2, a reporter (Sst2-GFP) that exhibits detectable binding only to the unphosphorylated form of the receptor, and a mutant form of Gα (Gpa1^{G302S}) that cannot interact with Sst2 (Ballon et al., 2006). Ste2^{7XR}-mCherry is uniformly distributed on the plasma membrane of vegetative YDB111 cells

and because it cannot be internalized, its localization does not change when YDB111 cells are treated with pheromone. In contrast, pheromone causes the Sst2-GFP reporter to concentrate on the plasma membrane of the mating projection, indicating a relatively high proportion of unphosphorylated receptor at the shmoo site (Ballon et al., 2006). This unexpected finding—more unphosphorylated receptor in the mating projection and more phosphorylated receptor at the back of the cell despite a uniform distribution of receptor overall—was attributed to a lag in the phosphorylation of nascent receptor recently delivered to the growth site. We tested this by treating G1-synchronized cultures of YDB111 cells with either pheromone, or pheromone + LatA, and then following the localization of Sst2-GFP over time (Figure 8). As reported previously (Ballon et al., 2006), Sst2-GFP polarized to the mating projection in cells treated with pheromone only (Figure 8, A and B). Remarkably, however, Sst2-GFP polarity was also observed in the pheromone + LatA-treated cells (Figure 8, A and B), which lacked detectable F-actin structures (Figure 8C), indicat-

Table 3. Receptor internalization is important for partner discrimination

Strain	Relevant genotype	RI[a]	Fold difference	Mating efficiency, %
DMY171	*ste2Δ URA3::STE2*	0.95×10^{-5}	N/A[b]	51.2
LHY848	*ste2Δ URA3::ste2-337R-340Stop*	9.08×10^{-3}	956	34.0
LHY844	*ste2Δ URA3::ste2-337R,340-UBIK48R*	1.66×10^{-2}	1747	12.3
LRB758	*YCK1 YCK2* at 23°C	3.2×10^{-6}	N/A	58.9
LRB758	*YCK1 YCK2* at 37°C	3.8×10^{-6}	N/A	61.1
LRB756	*Δyck1, yck2ts* at 23°C	4.8×10^{-6}	1.5	5.2
LRB756	*Δyck1, yck2ts* at 37°C	1.8×10^{-4}	47	0.7

[a] The randomness index (RI) was obtained by dividing the number of diploids formed with nonsecretors by the number of diploids formed with secretors (Schrick *et al.*, 1997).
[b] N/A, not applicable.

ing that pheromone can induce an asymmetric distribution of unphosphorylated receptor even in cells that can neither internalize the receptor nor polarize its secretion. In other words, in cells unable to polarize the receptor, phosphorylation was nevertheless asymmetric. It is well established that phosphorylation of the receptor triggers its endocytosis (Hicke *et al.*, 1998). Thus, if the asymmetrical distribution of phosphorylated receptor seen here occurs in wild-type cells, it must necessarily lead to an asymmetry in receptor internalization, consistent with the postulated positive feedback loop. Presumably, asymmet-

ric phosphorylation of the receptor would be detectable much earlier in the response of cells able to internalize the receptor and to polarize their secretion. The interaction between Gpa1 and Sst2, which is blocked by mutation in YDB111 cells, is also likely to play a role in feedback amplification of the growth site. We conclude that polarity could be established during the actin-dependent phase of the response by a mechanism involving differential phosphorylation and internalization of the receptor, as well as by established mechanisms such as Cdc42-driven symmetry breaking (Kozubowski *et al.*, 2008).
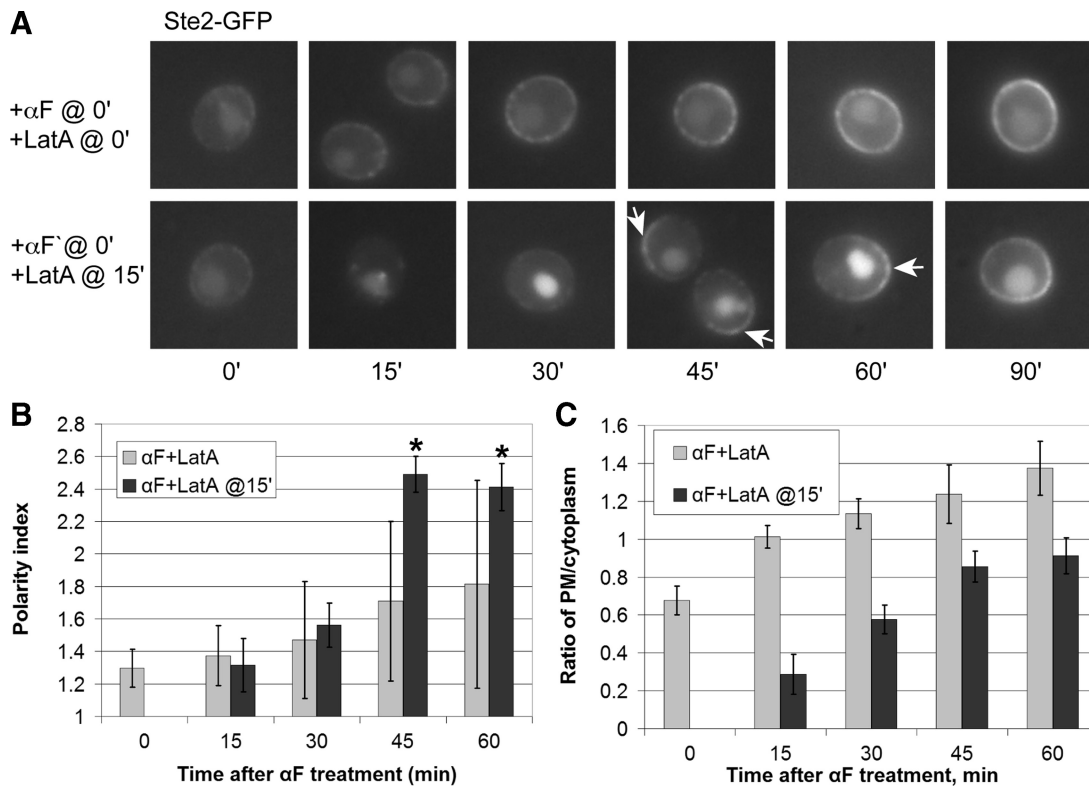

Figure 7. Polarization of nascent Ste2-GFP does not require polymerized actin after internalization has cleared the preexisting Ste2-GFP signal from the membrane. (A) Representative fluorescent images of Ste2-GFP localization in pheromone- and LatA-treated wild-type cells. G1-synchronized DMY169 cells were either concomitantly treated with 30 nM pheromone and 200 μM LatA (top row), or the LatA dose was added 15 min after pheromone treatment (bottom row). Images were acquired every 15 min. Arrows indicate Ste2-GFP crescents. (B) Quantification of Ste2-GFP polarization. The bar graphs represent the mean polarity index $\pm$ SD at each time point (n = 15). *p < 0.0001 for the comparisons of treated cells to 0 min. (C) Ratio of plasma membrane to intracellular Ste2-GFP signal. The bar graphs represent the mean ratio $\pm$ SD of the plasma membrane to cytoplasmic signals at each time point (n = 15).
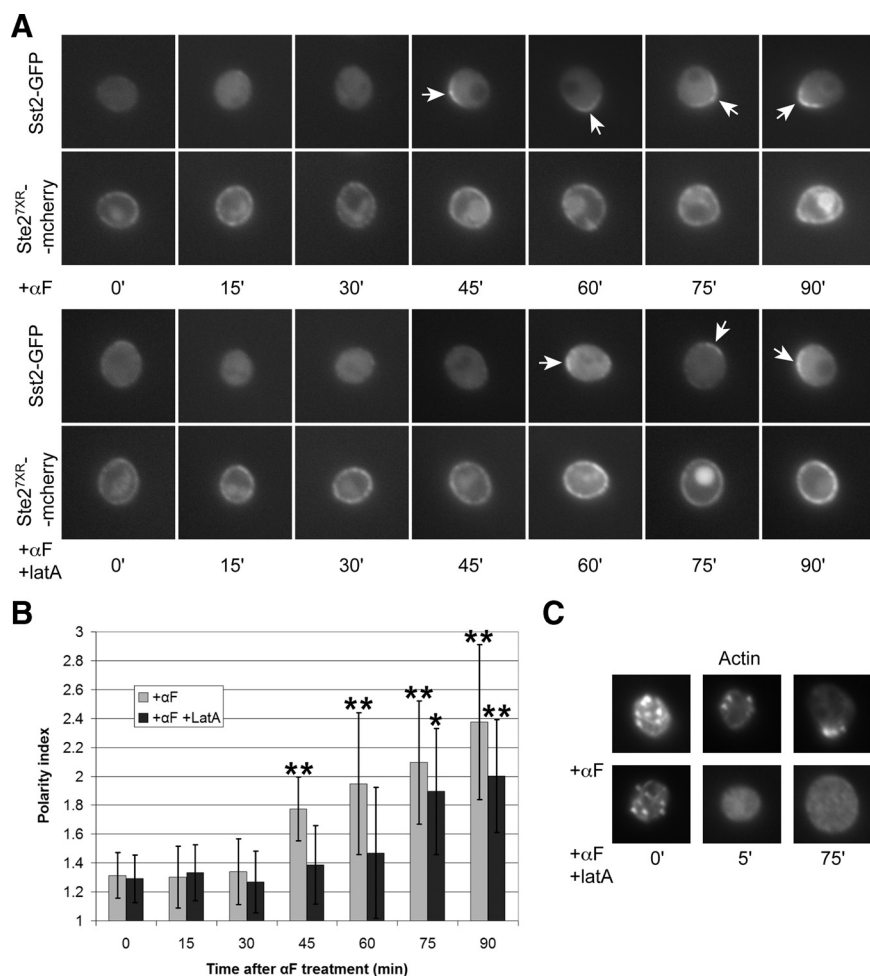
Figure 8. Pheromone induces asymmetric receptor phosphorylation in cells unable to polarize the receptor. (A) G1-synchronized YDB111 cells, which express a reporter that specifically binds to the unphosphorylated form of the receptor (Sst2-GFP) and a form of the receptor that cannot be internalized (Ste2^{7XR}-mCherry), were treated with 1.2 μM pheromone (top) or with 1.2 μM pheromone and 200 μM LatA (bottom). Images were acquired every 15 min. Arrows indicate the polarized localization of Sst2-GFP. (B) Quantification of Sst2-GFP polarization. The Sst2-GFP polarity indices were obtained as described in the legend to Figure 2. The bar graphs represent the mean polarity index $\pm$ SD at each time point (n = 15). *p < 0.001 and **p < 0.0002 for the comparisons of treated to untreated cells at each time point. (C) Effect of LatA on F-actin in YDB111 cells. Representative cells treated with pheromone and LatA at 0 time as described in A are shown. F-actin structures were not detectable at the 5- and 75-min time points.

Pheromone-induced Polarization of Gα Depends on Receptor Internalization and Receptor–Gα Contact

Like the pheromone receptor, the Gα and G$\beta\gamma$ subunits of the mating-specific G protein polarize on the plasma membrane in response to pheromone treatment (Kim *et al.*, 2000; Zaichick *et al.*, 2009). To elucidate the mechanisms underlying G protein polarization, we again evaluated the effects of various genetic manipulations on the localization of GFP-tagged reporters.

Wild-type cells expressing Gpa1 (Gα) tagged with GFP in situ were synchronized in G1, and Gpa1-GFP localization was quantified in vegetative and pheromone-treated cultures (Figure 9). We made two surprising observations in this experiment. First, the localization of Gpa1-GFP was cell cycle dependent. Although the reporter was uniformly distributed around the plasma membrane of G1 cells, it clearly polarized to the presumptive bud site at bud emergence (Figure 9, A and C), and accumulated at the mother-daughter neck in G2 and M (data not shown). Second, the amount of Gpa1-GFP on the plasma membrane decreased during the first 15 min of pheromone treatment (Figure 9A). The loss of Gpa1-GFP signal at the membrane was not complete, as in the case of Ste2-GFP, but it was easily perceptible and statistically significant (Figure 9D). As reported previously (Zaichick *et al.*, 2009), we also found that pheromone induced polarized localization of Gpa1-GFP to the presumptive shmoo site before any obvious change in cell morphology (Figure 9, A and C). The kinetics of Gpa1-GFP

internalization and polarization were similar to those of Ste2-GFP, and the sizes of the Gα and receptor crescents as a proportion of cell circumference also seemed to be about the same.

A priori, the pheromone-induced reduction in the Gpa1-GFP signal at the plasma membrane could be due to decreased delivery of Gpa1 to the membrane, a plasma membrane specific increase in Gpa1 turnover, dissociation of Gpa1 from the plasma membrane, and/or to increased Gpa1 internalization. Given that pheromone induces receptor internalization and that the receptor physically interacts with Gpa1, we wondered whether the receptor and its G protein are internalized together. To test this, we assessed the effect of pheromone treatment on the localization of Gpa1-GFP in a Ste2$^{K337R/340Stop}$ strain. Significantly, pheromone treatment did not cause a diminution of the Gpa1-GFP signal at the plasma membrane in cells unable to internalize their receptor (Figure 9E). Moreover, there was no evidence of Gpa1 polarization before morphogenesis, although Gpa1 polarity was observed in shmooing cells (Figure 9E). If Gpa1 and the receptor are cointernalized, is it simply because they are proximal on the membrane or because they are physically coupled? To answer this question, we followed the localization of a Gpa1 reporter that is unable to interact with the receptor, Gpa1$^{CT\Delta5}$-GFP (Hirsch *et al.*, 1991), in *gpa1Δ* cells. Although the mutant Gpa1 reporter localized normally to the plasma membrane of vegetative cells, pheromone did not effect any change in its distribution
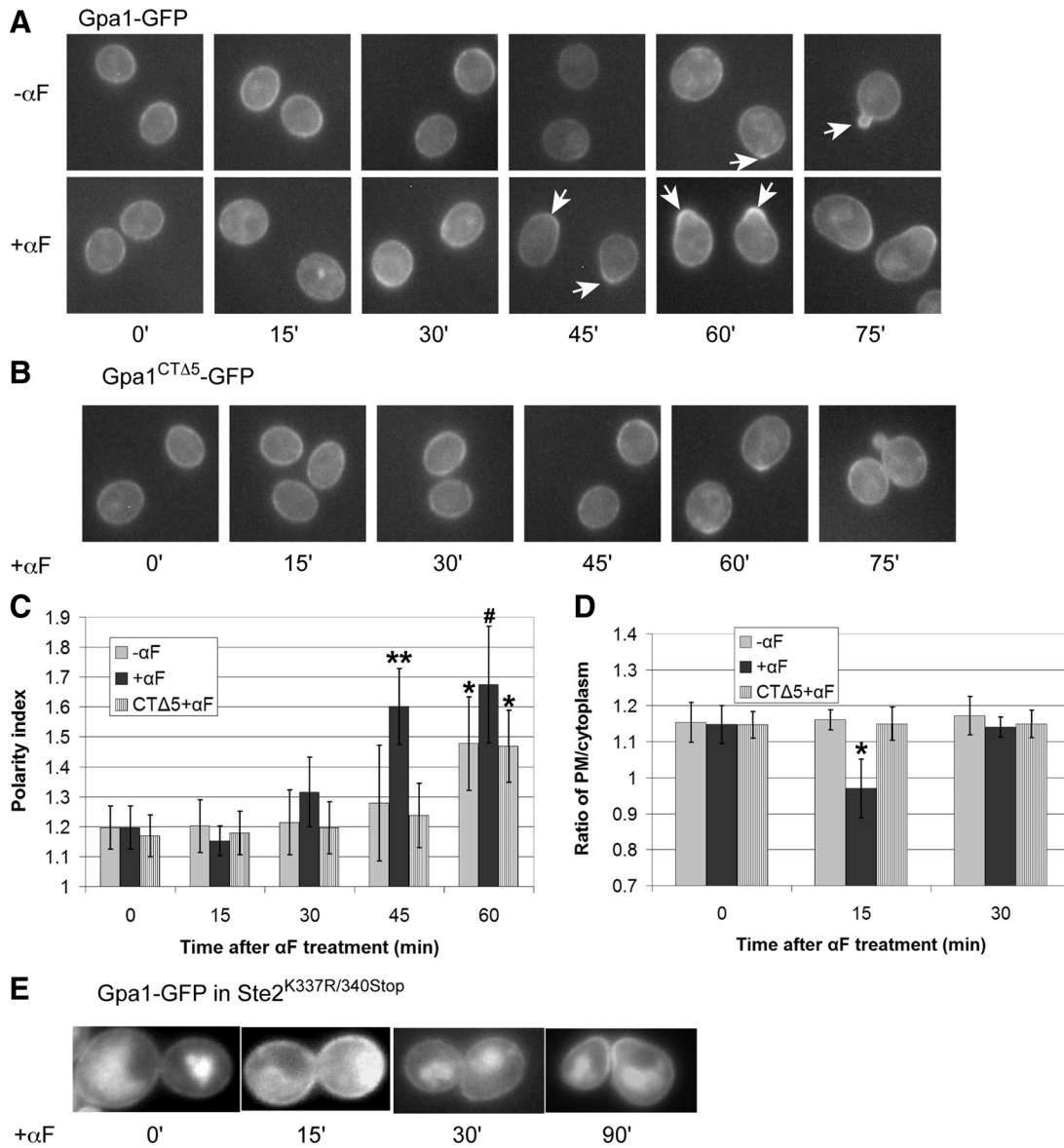
Figure 9. Pheromone-induced internalization and polarization of Gα (Gpa1) (A) Representative fluorescent images of Gpa1-GFP localization in wild type strain DSY257. G1-synchronized cells were treated with 30 nM pheromone (0 time) or cultured without pheromone, and images were acquired every 15 min. Arrows indicate Gpa1-GFP crescents. (B) Representative fluorescent images of Gpa1^{CTΔ5}-GFP localization in *gpa1Δ* strain DMY238. G1-synchronized cells expressing Gpa1^{CTΔ5}-GFP from a centromeric plasmid were treated with 30 nM pheromone (0 time), and images were acquired every 15 min. (C) Quantification of Gpa1-GFP and Gpa1^{CTΔ5}-GFP polarization. The bar graphs represent the mean polarity index ± SD at each time point (n = 15). The Gpa1-GFP reporter displayed significant cell cycle dependent polarization in untreated cells (*p < 0.0001 for the comparison to 0 min) and polarized dramatically in response to the pheromone (**p < 0.0001 compared with 0 min and p < 0.0001 compared untreated cells at 45 min; #p < 0.0001 compared with 0 min and p < 0.01 compared with untreated cells at 60 min). Gpa1^{CTΔ5}-GFP localization in treated cells was similar to Gpa1-GFP in untreated cells at all time points. (D) Ratio of Gpa1-GFP and Gpa1^{CTΔ5}-GFP plasma membrane to intracellular reporter signals. The bar graphs represent the mean ratio ± SD of the plasma membrane to cytoplasmic signals at each time point (n = 15). *p < 0.0001 for the comparison treated to untreated cells. (E) Pheromone-induced Gα internalization and early polarization depends on receptor internalization. A mid-log phase culture of Ste2$^{K337R/340Stop}$ cells expressing Gpa1-GFP from a centromeric plasmid were treated with 30 nM pheromone (0 time) and imaged at the indicated time points. Representative fluorescent images are shown. None of the cells examined showed clear evidence of Gpa1-GFP internalization (n ≥ 50).

(Figure 9, B–D). Presuming that pheromone induces internalization of the wild-type receptor in this strain, this implies that Gpa1 must contact the receptor to be internalized. It is unlikely that uncoupling Gpa1 from the receptor prevents the internalization of both molecules, as receptor internalization is triggered by ligand binding and does not depend on the G protein (Zanolari *et al.*, 1992). Together, these data suggest that pheromone in-

duces the internalization of Gpa1 via its contact with the receptor, and that this is a requisite step in Gpa1 polarization during the mating response.

Pheromone-induced Polarization of Gβ Depends on Receptor Internalization and Functional Gα

The putative coupling of receptor and Gα internalization suggested to us the possibility that the entire signaling unit—the

Figure 10. Pheromone-induced internalization and polarization of Gβ (Ste4). (A) Representative fluorescent images of GFP-Ste4 localization in the wild type strain DSY257. G1-synchronized cells were treated with 30 nM pheromone (0 time) or cultured without pheromone and images were acquired every 15 min. Arrows indicate GFP-Ste4 crescents. (B) Quantification of GFP-Ste4 polarization. The bar graphs represent the mean polarity index ± SD at each time point (n = 15). The GFP-Ste4 reporter displayed significant cell cycle dependent localization in untreated cells, concentrating at the incipient bud site and at the mother-daughter neck, and polarized dramatically in response to the pheromone (*p < 0.0001 compared with 0 min and p < 0.001 compared with the same time point in untreated cells; **p < 0.0001 compared with the same time point in untreated cells). (C) Ratio of GFP-Ste4 plasma membrane to intracellular signals. The bar graphs represent the mean ratio ± SD of the plasma membrane to cytoplasmic signals at each time point (n = 15). (*p < 0.001 compared with the same time point in untreated cells). (D) Pheromone-induced Gβ internalization and early polarization depends on receptor internalization. A mid-log phase culture of Ste2[K337R/340Stop] cells expressing GFP-Ste4 from a centromeric plasmid were treated with 30 nM pheromone (0 time) and imaged at the indicated time points. Representative fluorescent images are shown. None of the cells examined showed clear evidence of GFP-Ste4 internalization (n ≥ 50). (E) Pheromone-induced Gβ internalization and polarization depends on Gpa1. A mid-log phase culture of gpa1[ts] cells expressing GFP-Ste4 from a centromeric plasmid were treated with 30 nM pheromone at the permissive temperature (0 time for the 23°C cultures) or 5 min after the shift to restrictive temperature (0 time for the 37°C cultures) and imaged at the indicated time points. Representative fluorescent images are shown. None of the cells examined showed evidence of GFP-Ste4 internalization (n ≥ 50).
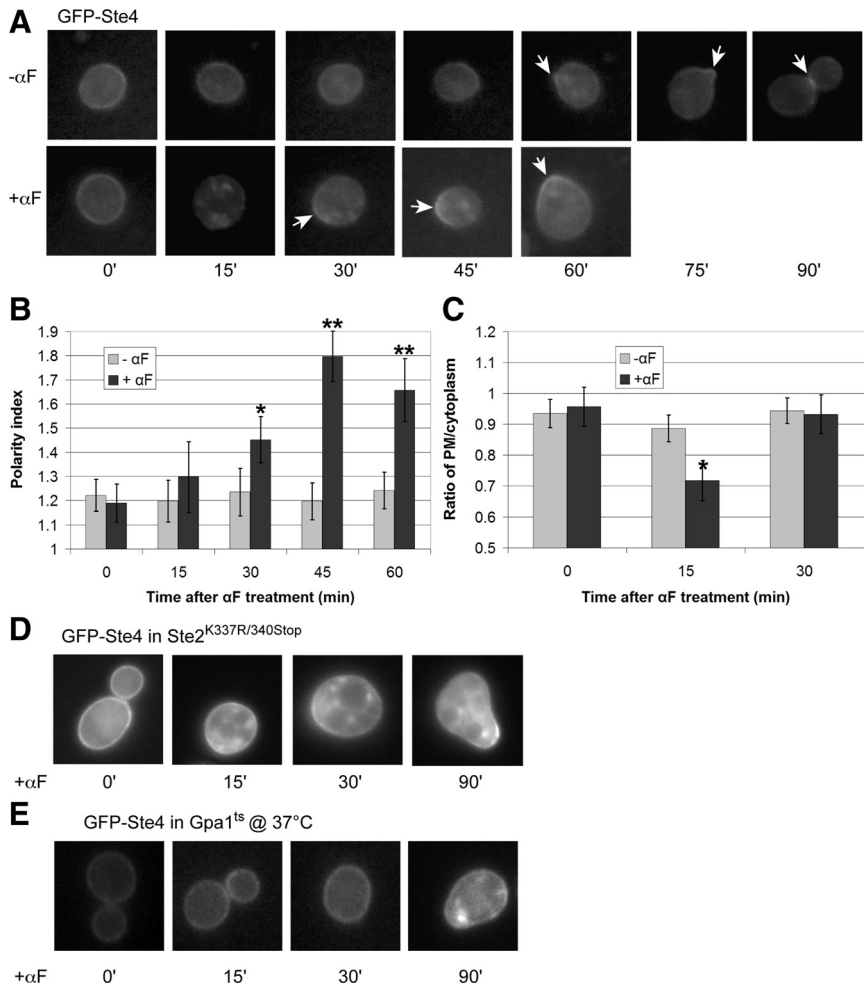
GPCR and its heterotrimeric G protein—are removed from the plasma membrane as part of one concerted mechanism. To determine whether Gβγ might internalize and polarize along with Gα and the receptor, we assayed the localization of GFP-tagged Ste4 (Gβ) expressed in wild-type, Ste2[K337R/340Stop], and gpa1[ts] cells. In G1-synchronized wild-type cells, GFP-Ste4 exhibited a cell cycle dependent localization similar to that of Gpa1-GFP—uniform on the plasma membrane in G1, concentrated at the presumptive bud site around bud emergence, on the plasma membrane of small buds, and at the mother-daughter neck in M and G2 (Figure 10A)—although the overall GFP-Ste4 signal in vegetatively growing cells was much weaker than that of Gpa1-GFP, presumably due to a lower expression level (Ghaemmaghami et al., 2003). Pheromone treatment of these cells elicited changes in GFP-Ste4 localization that were similar to the signal-induced changes in Gpa1 and Ste2 localization—the Gβ reporter largely disappeared from the plasma membrane after 15 min of stimulation but reemerged as a polarized crescent 15 min after that (Figure 10, A–C). Moreover, GFP-Ste4 did not internalize in pheromone-treated Ste2[K337R/340Stop] cells or in cells lacking functional Gpa1, and it showed little or no polarity before shmoo formation in Ste2[K337R/340Stop] and gpa1-null cells, respectively (Figure 10, D and E). Together, these data suggest that pheromone induces the internalization of Gβγ via its contact with Gα, and that this is essential for the initial polarization of Gβγ (i.e., before its polarized secretion) during the mating response.

DISCUSSION

Actin-dependent directed secretion and internalization have been invoked to explain the polarization of several molecules that are trafficked to the yeast cell surface (Valdez-Taubas and Pelham, 2003; Proszynski et al., 2006). According to this paradigm, such molecules are delivered to the growth site along oriented actin cables and endocytosed at a rate that prevents the loss of polarity due to diffusion (Valdez-Taubas and Pelham, 2003). To determine whether receptor polarization could help establish the growth site or is simply the result of directed secretion during the yeast mating response, we examined the consequences of perturbing these processes on receptor localization. For convenience, we studied the mechanisms underlying receptor polarization in cells subjected to isotropic pheromone stimulation.

Receptor Polarization Precedes Directed Secretion along Actin Cables

Several of our observations suggest that the establishment of receptor polarity does not require actin-dependent directed secretion: 1) Receptor polarization was detected before the appearance of polarized actin cables and before an obvious change in cell shape. 2) Receptor crescents can form in the absence of Myo2 and tropomyosin function. 3) Pheromone-treated cells can form robust receptor crescents in the absence of F-actin once they have internalized the receptor to

the point that we cannot detect it on the membrane. These results can be explained by invoking the biased fusion of vesicles containing Ste2-GFP (Sahin *et al.*, 2008) to a polarization site established via symmetry breaking at the level of the Cdc42 guanine nucleotide exchange factor (GEF)—p21-activated kinase (PAK) complex (Kozubowski *et al.*, 2008). It has been demonstrated that in the absence of F-actin, secretory vesicles preferentially dock and fuse where polarity cues are localized in cells exiting quiescence (Sahin *et al.*, 2008) and that *bni1 bnr1* mutant cells, which lack actin cables at restrictive temperature, can nevertheless form small buds (Bettinger *et al.*, 2007; Yamamoto *et al.*, 2010). Like the receptor, Cdc42 polarizes (albeit transiently) in *myo2-16* and *tpm1-2 tpm2Δ* cells at restrictive temperature (Irazoqui *et al.*, 2005). Polarization of the receptor might also be driven by its tendency to form dimers (Overton and Blumer, 2000) and oligomers (Wang and Konopka, 2009), or by local changes in the composition of the plasma membrane that could attract or stabilize the receptor clusters (Bagnat and Simons, 2002; Proszynski *et al.*, 2006).

Our data can also be explained by a second, more speculative model. In principle, receptor polarity could be established upon pheromone stimulation without any dependence on cable-directed secretion if internalization of the receptor were slower on one side of the cell than the other. Because Yck-dependent phosphorylation of the receptor triggers its internalization, this hypothesis correctly predicts our observations that cells lacking Yck function or that are otherwise unable to internalize the receptor cannot polarize the receptor and that pheromone induces asymmetric phosphorylation of uniformly distributed receptors. How might asymmetry in the phosphorylation and internalization of the receptor arise? One possibility is that the G protein—either Gα or G$\beta\gamma$—inhibits phosphorylation of the receptor. Gα and Gβ both concentrate at the cortex of the presumptive bud site (Figures 9A and 10A), which becomes the default mating projection site when cells are subjected to isotropic pheromone treatment, and like the Cdc42 GEF–PAK complex, may be subject to symmetry breaking mechanisms. An initially slight accumulation of Gα and G$\beta\gamma$ at a distinct cortical site would result in more receptors and G protein being left at that site, thereby creating a positive feedback loop that would rapidly amplify the localized signal. The coupling of G protein and receptor internalization that our data imply (Figures 9, D and E, and 10, D and E) should further augment the amplification power of this loop because the entire signaling unit is either removed or left on the membrane, and in the latter case, the density of the putative receptor protector element (Gα or G$\beta\gamma$) would increase along with the density of the receptor. We imagine that these amplification mechanisms begin to induce asymmetric receptor phosphorylation and distribution immediately upon pheromone stimulation, long before we can detect Ste2-GFP or Sst2-GFP crescents. Note that the delay in the appearance of the Sst2-GFP crescent (45′) relative to that of the Ste2-GFP crescent (30′) is not surprising given that the receptor phosphorylation assay is performed in cells that cannot internalize the receptor and which therefore lack the postulated primary amplification loop. Similarly, it is not surprising that the LatA-treated cells took an additional fifteen minutes to form Sst2-GFP crescents given their inability to polarize secretion via actin cables.

As yet, our data do not allow us to determine whether cable-independent receptor polarity is driven by symmetry breaking and biased docking, receptor protection and differential internalization, a combination of the two mechanisms, or neither mechanism.

Role of the Casein Kinases

The data shown in Figure 7 indicate that a precursor to detectable receptor polarity is established by actin-dependent mechanisms in the first 15 min of pheromone treatment, after which the polarized receptor crescent can emerge in the absence of polymerized actin. In contrast, receptor crescents cannot form without ongoing Yck activity even if they are allowed to internalize the receptor for 15 min before Yck activity is abolished (Figure 6). This implies that Yck provides a function essential to the generation of receptor polarity in addition to the triggering of receptor internalization. The proposed role of the heterotrimeric G protein in the protection of the receptor from phosphorylation and internalization might provide the key to understanding this observation. In mammalian cells, ligand-induced phosphorylation of GPCRs disrupts receptor-G protein interaction (reviewed in Ferguson, 2001). If phosphorylation of the yeast pheromone receptor also uncouples it from its G protein, then localized inhibition of Yck by Gα or G$\beta\gamma$ would lead to a patch of unphosphorylated receptor, which, unlike the phosphorylated receptor, would be competent to recruit G protein to the incipient polarization site, thus augmenting protection of the receptor in a positive feedback loop. Generation of the pheromone-induced Sst2-GFP crescent (Figure 8), which represents a localized con-
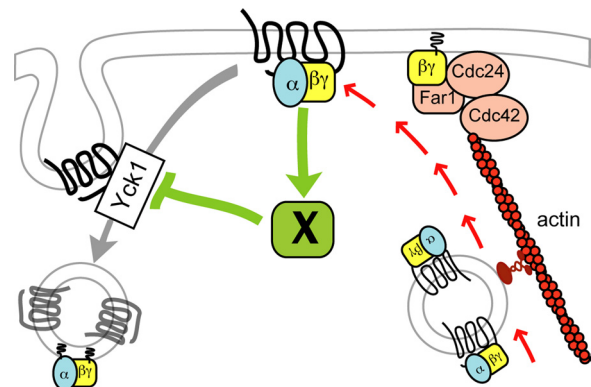

Figure 11. Induction of receptor polarity by differential receptor internalization. The cartoon illustrates a putative positive feedback loop that accounts for the cell's ability to polarize the pheromone receptor and its G protein before their localized deposition by actin-dependent directed secretion. We postulate that the initially slight gradient of activated receptor and G protein activates and/or recruits an unknown factor (X) that protects ligand-bound receptors from Yck-dependent phosphorylation, thereby inhibiting receptor and G protein internalization. This increases the local concentration of receptor and G protein at the future shmoo site which further stimulates the protective activity of factor X. Eventually, there is a sufficient concentration of G$\beta\gamma$ to define the axis of polarity via recruitment of the Far1–Cdc24–Cdc42 chemotropic complex. This model provides an explanation both for directional sensing in a pheromone gradient and symmetry breaking under isotropic conditions and is consistent with our major findings: 1) Pheromone-induced receptor polarization is absolutely dependent on receptor internalization but can occur in absence of actin-dependent directed secretion. 2) The receptor polarizes before detectable polarization of actin cables and morphogenesis. 3) Polarized receptor crescents are invariably oriented toward potential mating partners when they first appear. 4) Pheromone treatment of cells forced to maintain a uniform distribution of receptor induces hypophosphorylated receptor crescents. We believe G$\beta\gamma$ is a good candidate to be factor X, as we have found that Gβ physically interacts with Yck1 (Stone and Ismael, unpublished data). Note that the coupled delivery of the receptor and G protein to the growth site is purely speculative.

centration of unphosphorylated receptor, may partially depend on such a loop. Further analysis will be required to fully elucidate the role of the casein kinases in the generation of receptor polarity.

Implications for Gradient Sensing

A key question about the yeast chemotropic response—indeed about chemotropic systems in general—is how a very slight gradient of activated receptor can define the site of polarized growth. We show here that in mating mixtures, the detectable receptor crescents are invariably oriented toward the closest mating partner (Figure 1) and that disrupting receptor internalization and polarization correlates with severe defects in directional sensing (Table 3). Others have shown that the C-terminal cytoplasmic domain of the receptor, which contains the phosphorylation and ubiquitination sites, is essential for mating projection orientation in artificial pheromone gradients (Vallier *et al.*, 2002). These observations are consistent with a role for receptor polarization in directional sensing. Because the receptor crescent is observed before the polarization of actin cables and does not require actin-dependent directed secretion, we postulate that in pheromone gradients, receptor polarization determines the axis of polarity and is not simply the result of polarized secretion.

Although chemotropic polarization cannot be equated with default polarization, pheromone-induced redistribution of the receptor in liquid cultures was indistinguishable from that observed in mating mixtures and was unaffected by the absence of Bud1. Additional experiments will be required to determine whether the receptor is indeed polarized by differential internalization and whether this contributes to directional sensing. Nevertheless, our findings do suggest a mechanism by which receptor polarity could be established and the polarization site properly positioned in a pheromone gradient before the initiation of directed secretion. We propose that the activated receptor stimulates a downstream element or elements that protect it from internalization. The receptor is therefore endocytosed less efficiently where there is a higher density of activated receptors, i.e., on the up-gradient side of the cell (Figure 11). This causes more receptor and G protein to be left on the membrane, which increases signaling to the downstream protective element, and so on until the localized concentration of receptor and G protein is sufficient to establish the axis of polarity. Nucleation/polarization of actin cables and directed secretion then stabilize and amplify signaling at the incipient growth site.

ACKNOWLEDGMENTS

REFERENCES

Ausubel, F. M., Brent, R., Kingston, R. E., Moore, D. D., Seidman, J. G., Smith, J. A., and Struhl, K. (1994). Current Protocols in Molecular Biology. John Wiley & Sons, New York, NY.

Ayscough, K. R., and Drubin, D. G. (1998). A role for the yeast actin cytoskeleton in pheromone receptor clustering and signalling. Curr. Biol. *8*, 927–930.

Bagnat, M., and Simons, K. (2002). Cell surface polarization during yeast mating. Proc. Natl. Acad. Sci. USA *99*, 14183–14188.

Ballon, D. R., Flanary, P. L., Gladue, D. P., Konopka, J. B., Dohlman, H. G., and Thorner, J. (2006). DEP-domain-mediated regulation of GPCR signaling responses. Cell *126*, 1079–1093.

Basile, J. R., Barac, A., Zhu, T., Guan, K. L., and Gutkind, J. S. (2004). Class IV semaphorins promote angiogenesis by stimulating Rho-initiated pathways through plexin-B. Cancer Res. *64*, 5212–5224.

Bettinger, B. T., Clark, M. G., and Amberg, D. C. (2007). Requirement for the polarisome and formin function in Ssk2p-mediated actin recovery from osmotic stress in *Saccharomyces cerevisiae*. Genetics *175*, 1637–1648.

Biber, K., Zuurman, M. W., Dijkstra, I. M., and Boddeke, H. W. (2002). Chemokines in the brain: neuroimmunology and beyond. Curr. Opin. Pharmacol. *2*, 63–68.

Brachmann, C. B., Davies, A., Cost, G. J., Caputo, E., Li, J., Hieter, P., and Boeke, J. D. (1998). Designer deletion strains derived from *Saccharomyces cerevisiae* S288C: a useful set of strains and plasmids for PCR-mediated gene disruption and other applications. Yeast *14*, 115–132.

Daniels, K. J., Srikantha, T., Lockhart, S. R., Pujol, C., and Soll, D. R. (2006). Opaque cells signal white cells to form biofilms in *Candida albicans*. EMBO J. *25*, 2240–2252.

Dorer, R., Pryciak, P. M., and Hartwell, L. H. (1995). *Saccharomyces cerevisiae* cells execute a default pathway to select a mate in the absence of pheromone gradients. J. Cell Biol. *131*, 845–861.

Dunn, R., Klos, D. A., Adler, A. S., and Hicke, L. (2004). The C2 domain of the Rsp5 ubiquitin ligase binds membrane phosphoinositides and directs ubiquitination of endosomal cargo. J. Cell Biol. *165*, 135–144.

English, D., Garcia, J. G., and Brindley, D. N. (2001). Platelet-released phospholipids link haemostasis and angiogenesis. Cardiovasc. Res. *49*, 588–599.

Evangelista, M., Pruyne, D., Amberg, D. C., Boone, C., and Bretscher, A. (2002). Formins direct Arp2/3-independent actin filament assembly to polarize cell growth in yeast. Nat. Cell Biol. *4*, 260–269.

Ferguson, S. S. (2001). Evolving concepts in G protein-coupled receptor endocytosis: the role in receptor desensitization and signaling. Pharmacol. Rev. *53*, 1–24.

Ghaemmaghami, S., Huh, W. K., Bower, K., Howson, R. W., Belle, A., Dephoure, N., O'Shea, E. K., and Weissman, J. S. (2003). Global analysis of protein expression in yeast. Nature *425*, 737–741.

Gietz, R. D., and Sugino, A. (1988). New yeast-*Escherichia coli* shuttle vectors constructed with in vitro mutagenized yeast genes lacking six-base pair restriction sites. Gene *74*, 527–534.

Gordon, A., Colman-Lerner, A., Chin, T. E., Benjamin, K. R., Yu, R. C., and Brent, R. (2007). Single-cell quantification of molecules and rates using open-source microscope-based cytometry. Nat. Methods *4*, 175–181.

Hicke, L., Zanolari, B., and Riezman, H. (1998). Cytoplasmic tail phosphorylation of the alpha-factor receptor is required for its ubiquitination and internalization. J. Cell Biol. *141*, 349–358.

Hirsch, J. P., Dietzel, C., and Kurjan, J. (1991). The carboxyl terminus of Scg1, the Gα subunit involved in yeast mating, is implicated in interactions with the pheromone receptors. Genes Dev. *5*, 467–474.

Iijima, M., Huang, Y. E., and Devreotes, P. (2002). Temporal and spatial regulation of chemotaxis. Dev. Cell *3*, 469–478.

Irazoqui, J. E., Howell, A. S., Theesfeld, C. L., and Lew, D. J. (2005). Opposing roles for actin in Cdc42p polarization. Mol. Biol. Cell *16*, 1296–1304.

Jackson, C. L., and Hartwell, L. H. (1990). Courtship in *Saccharomyces cerevisiae*: an early cell-cell interaction during mating. Mol. Cell Biol. *10*, 2202–2213.

Jackson, C. L., Konopka, J. B., and Hartwell, L. H. (1991). *S. cerevisiae* alpha pheromone receptors activate a novel signal transduction pathway for mating partner discrimination. Cell *67*, 389–402.

Jenness, D. D., and Spatrick, P. (1986). Down regulation of the α-factor pheromone receptor in *S. cerevisiae*. Cell *46*, 345–353.

Kim, J., Bortz, E., Zhong, H., Leeuw, T., Leberer, E., Vershon, A. K., and Hirsch, J. P. (2000). Localization and signaling of Gβ subunit Ste4p are controlled by a-factor receptor and the a-specific protein Asg7p. Mol. Cell Biol. *20*, 8826–8835.

Kim, S., Dong, J., and Lord, E. M. (2004). Pollen tube guidance: the role of adhesion and chemotropic molecules. Curr. Top. Dev. Biol. *61*, 61–79.

Konopka, J. B., Jenness, D. D., and Hartwell, L. H. (1988). The C-terminus of the *S. cerevisiae* α-pheromone receptor mediates an adaptive response to pheromone. Cell *54*, 609–620.

Kozubowski, L., Saito, K., Johnson, J. M., Howell, A. S., Zyla, T. R., and Lew, D. J. (2008). Symmetry-breaking polarization driven by a Cdc42p GEF-PAK complex. Curr. Biol. *18*, 1719–1726.

Liu, J. J., and Lindquist, S. (1999). Oligopeptide-repeat expansions modulate 'protein-only' inheritance in yeast. Nature *400*, 573–576.

Mato, J. M., Losada, A., Nanjundiah, V., and Konijn, T. M. (1975). Signal input for a chemotactic response in the cellular slime mold *Dictyostelium discoideum*. Proc. Natl. Acad. Sci. USA 72, 4991–4993.

McNulty, J. J., and Lew, D. J. (2005). Swe1p responds to cytoskeletal perturbation, not bud size, in *S. cerevisiae*. Curr. Biol. *15*, 2190–2198.

Metodiev, M. V., Matheos, D., Rose, M. D., and Stone, D. E. (2002). Regulation of MAPK function by direct interaction with the mating-specific Gα in yeast. Science *296*, 1483–1486.

Moore, T. I., Chou, C. S., Nie, Q., Jeon, N. L., and Yi, T. M. (2008). Robust spatial sensing of mating pheromone gradients by yeast cells. PLoS ONE *3*, e3865.

Nern, A., and Arkowitz, R. A. (1999). A Cdc24p-Far1p-Gβγ protein complex required for yeast orientation during mating. J. Cell Biol. *144*, 1187–1202.

Overton, M. C., and Blumer, K. J. (2000). G-protein-coupled receptors function as oligomers in vivo. Curr. Biol. *10*, 341–344.

Palanivelu, R., and Preuss, D. (2000). Pollen tube targeting and axon guidance: parallels in tip growth mechanisms. Trends Cell Biol. *10*, 517–524.

Panek, H. R., Stepp, J. D., Engle, H. M., Marks, K. M., Tan, P. K., Lemmon, S. K., and Robinson, L. C. (1997). Suppressors of YCK-encoded yeast casein kinase 1 deficiency define the four subunits of a novel clathrin AP-like complex. EMBO J. *16*, 4194–4204.

Pringle, J. R., Preston, R. A., Adams, A. E., Stearns, T., Drubin, D. G., Haarer, B. K., and Jones, E. W. (1989). Fluorescence microscopy methods for yeast. Methods Cell Biol. *31*, 357–435.

Proszynski, T. J., Klemm, R., Bagnat, M., Gaus, K., and Simons, K. (2006). Plasma membrane polarization during mating in yeast cells. J. Cell Biol. *173*, 861–866.

Pruyne, D., and Bretscher, A. (2000a). Polarization of cell growth in yeast. J. Cell Sci. *113*, 571–585.

Pruyne, D., and Bretscher, A. (2000b). Polarization of cell growth in yeast. I. Establishment and maintenance of polarity states. J. Cell Sci. *113*, 365–375.

Pruyne, D. W., Schott, D. H., and Bretscher, A. (1998). Tropomyosin-containing actin cables direct the Myo2p-dependent polarized delivery of secretory vesicles in budding yeast. J. Cell Biol. *143*, 1931–1945.

Rasband, W. S. (1997–2009). ImageJ. U.S. National Institutes of Health, Bethesda, MD. http://rsb.info.nih.gov/ij/.

Reneke, J. E., Blumer, K. J., Courchesne, W. E., and Thorner, J. (1988). The carboxy-terminal segment of the yeast alpha-factor receptor is a regulatory domain. Cell *55*, 221–234.

Rohrer, J., Benedetti, H., Zanolari, B., and Riezman, H. (1993). Identification of a novel sequence mediating regulated endocytosis of the G protein-coupled alpha-pheromone receptor in yeast. Mol. Biol. Cell *4*, 511–521.

Rubel, E. W., and Cramer, K. S. (2002). Choosing axonal real estate: location, location, location. J. Comp. Neurol. *448*, 1–5.

Sagot, I., Klee, S. K., and Pellman, D. (2002). Yeast formins regulate cell polarity by controlling the assembly of actin cables. Nat. Cell Biol. *4*, 42–50.

Sahin, A., Daignan-Fornier, B., and Sagot, I. (2008). Polarized growth in the absence of F-actin in *Saccharomyces cerevisiae* exiting quiescence. PLoS One *3*, e2556.

Schott, D., Ho, J., Pruyne, D., and Bretscher, A. (1999). The COOH-terminal domain of Myo2p, a yeast myosin V, has a direct role in secretory vesicle targeting. J. Cell Biol. *147*, 791–808.

Schrick, K., Garvik, B., and Hartwell, L. H. (1997). Mating in *Saccharomyces cerevisiae*: the role of the pheromone signal transduction pathway in the chemotropic response to pheromone. Genetics *147*, 19–32.

Segall, J. E. (1993). Polarization of yeast cells in spatial gradients of α mating factor. Proc. Natl. Acad. Sci. USA *90*, 8332–8336.

Servant, G., Weiner, O. D., Neptune, E. R., Sedat, J. W., and Bourne, H. R. (1999). Dynamics of a chemoattractant receptor in living neutrophils during chemotaxis. Mol. Biol. Cell *10*, 1163–1178.

Sheff, M. A., and Thorn, K. S. (2004). Optimized cassettes for fluorescent protein tagging in *Saccharomyces cerevisiae*. Yeast *21*, 661–670.

Sheltzer, J. M., and Rose, M. D. (2009). The class V myosin Myo2p is required for Fus2p transport and actin polarization during the yeast mating response. Mol. Biol. Cell *20*, 2909–2919.

Sherman, F., Fink, G. R., and Hicks, J. B., Eds. (1986). Laboratory Course Manual for Methods in Yeast Genetics, Cold Spring Harbor, NY: Cold Spring Harbor Laboratory Press.

Shih, S. C., Sloper-Mould, K. E., and Hicke, L. (2000). Monoubiquitin carries a novel internalization signal that is appended to activated receptors. EMBO J. *19*, 187–198.

Sikorski, R. S., and Hieter, P. (1989). A system of shuttle vectors and yeast host strains designed for efficient manipulation of DNA in *Saccharomyces cerevisiae*. Genetics *122*, 19–27.

Snetselaar, K. M., Bolker, M., and Kahmann, R. (1996). Ustilago maydis mating hyphae orient their growth toward pheromone sources. Fungal Genet. Biol. *20*, 299–312.

Terrell, J., Shih, S., Dunn, R., and Hicke, L. (1998). A function for monoubiquitination in the internalization of a G protein-coupled receptor. Mol. Cell *1*, 193–202.

Tranquillo, R. T., Lauffenburger, D. A., and Zigmond, S. H. (1988). A stochastic model for leukocyte random motility and chemotaxis based on receptor binding fluctuations. J. Cell Biol. *106*, 303–309.

Valdez-Taubas, J., and Pelham, H. R. (2003). Slow diffusion of proteins in the yeast plasma membrane allows polarity to be maintained by endocytic cycling. Curr. Biol. *13*, 1636–1640.

Vallier, L. G., Segall, J. E., and Snyder, M. (2002). The α-factor receptor C-terminus is important for mating projection formation and orientation in *Saccharomyces cerevisiae*. Cell Motil. Cytoskeleton *53*, 251–266.

Wach, A., Brachat, A., Alberti-Segui, C., Rebischung, C., and Philippsen, P. (1997). Heterologous HIS3 marker and GFP reporter modules for PCR-targeting in *Saccharomyces cerevisiae*. Yeast *13*, 1065–1075.

Wang, H. X., and Konopka, J. B. (2009). Identification of amino acids at two dimer interface regions of the alpha-factor receptor (Ste2). Biochemistry *48*, 7132–7139.

Weiner, O. D. (2002). Regulation of cell polarity during eukaryotic chemotaxis: the chemotactic compass. Curr. Opin. Cell Biol. *14*, 196–202.

Wiget, P., Shimada, Y., Butty, A. C., Bi, E., and Peter, M. (2004). Site-specific regulation of the GEF Cdc24p by the scaffold protein Far1p during yeast mating. EMBO J. *23*, 1063–1074.

Xiao, Z., Zhang, N., Murphy, D. B., and Devreotes, P. N. (1997). Dynamic distribution of chemoattractant receptors in living cells during chemotaxis and persistent stimulation. J. Cell Biol. *139*, 365–374.

Yamamoto, T., Mochida, J., Kadota, J., Takeda, M., Bi, E., and Tanaka, K. (2010). Initial polarized bud growth by endocytic recycling in the absence of actin cable-dependent vesicle transport in yeast. Mol. Biol. Cell *21*, 1237–1252.

Zaichick, S. V., Metodiev, M. V., Nelson, S. A., Durbrovskyi, O., Draper, E., Cooper, J. A., and Stone, D. E. (2009). The mating-specific Gα interacts with a kinesin-14 and regulates pheromone-induced nuclear migration in budding yeast. Mol. Biol. Cell *20*, 2820–2830.

Zanolari, B., Raths, S., Singer-Kruger, B., and Riezman, H. (1992). Yeast pheromone receptor endocytosis and hyperphosphorylation are independent of G protein-mediated signal transduction. Cell *71*, 755–763.

Zhang, X., Bi, E., Novick, P., Du, L., Kozminski, K. G., Lipschutz, J. H., and Guo, W. (2001). Cdc42 interacts with the exocyst and regulates polarized secretion. J. Biol. Chem. *276*, 46745–46750.